



# LIBRARY Michigan State University

This is to certify that the

THE BARRIER CHARACTERISTICS

OF CLAY/POLYIMIDE NANOCOMPOSITES

presented by

JIAJIAN GEORFIA GU

has been accepted towards fulfillment of the requirements for

MS. degree in PACKAGING

Date 4/23/97

Major professor

MSU is an Affirmative Action/Equal Opportunity Institution

PLACE IN RETURN BOX to remove this checkout from your record. TO AVOID FINES return on or before date due.

DATE DUE	DATE DUE	DATE DUE
All Q 9 mic		
NOV Q 2 1998		
JAN	7 <u>C</u> 2000	
1 MAR 1 6 2003		
0 MAR4 202 ₹00		
0 ( <u>152 8 2 00</u> 00		

MSU is An Affirmative Action/Equal Opportunity Institution cteirclassedus.pm3-p.

i

# THE BARRIER CHARACTERISTICS OF CLAY/POLYIMIDE NANOCOMPOSITES

Ву

Jiajian (Georgia) Gu

#### A THESIS

Submitted to
Michigan State University
in partial fulfillment of the requirements
for the degree of

MASTER OF SCIENCE

School of Packaging

1997

#### ABSTRACT

# THE BARRIER CHARACTERISTICS OF CLAY/POLYIMIDE NANOCOMPOSITES

By

Jiajian (Georgia) Gu

The permeability of water vapor, oxygen, carbon dioxide, and ethyl acetate vapor through clay/polyimide nanocomposite films was determined with the MOCON permeability testers. Factors affecting the barrier properties of clay/polyimide nanocomposites including: the clay loading level; the test temperature; the organic vapor concentration; and the relative humidity, were evaluated.

The incorporation of low loading levels of clay in the polyimide hybrid, resulted in a significant reduction in the permeability of the respective penetrants, as compared to the pure polyimide film. The results showed a non-linear dependence of permeability on clay loading. The temperature dependency of the transport processes, over the temperature ranges studied, followed well the Arrhenius relationship. The organic vapor concentration did not significantly affect the permeability coefficient. When tested under humidified conditions, the polyimide film showed a loss in barrier property, while the clay/polyimide film showed an enhancement in the barrier property to ethyl acetate.

To my dear family

#### **ACKNOWLEDGEMENTS**

I would like to express my heartfelt thanks to my major advisor Professor J. Giacin. His devoted and endless supports enabled me to complete this research. I would also like to thank Professor Hernandez and Professor Pinnavaia, for their precious advice and discussion throughout the course of this research. I also thank Dr. T. Lan and Dr. L. Rayas, for helping me to get started at many stages during the research. I also would thank people in MOCON (Modern Controls, Inc.), for their help, as well as their kind donation of the instrumentation. The research funding from CFMR (Center for Fundamental Materials Research) is also highly appreciated.

Finally, my family deserves to have my deepest thanks and love for their devoted supports during the research.

# TABLE OF CONTENTS

LIS	T OF T	ABLESviii
LIS	T OF F	IGURESx
INI	RODUC	TION1
LII		RE REVIEW
A.		Polymer Nanocomposites7
		oncepts of Composite and Nanocomposite Materials7
	2. R	ecent Approaches in Clay/Polymer Nanocomposites9
	3. T	he Barrier Properties of Clay/Polyimide anocomposites
в.	Conor	al Theory Related to the Permeation Process17
C.		rs Affecting the Permeability Properties of
•	I uc co.	Polymers21
D.	Model	s for the Permeability of Filled Polymers24
E.	Perme	ability Measurement Methods26
		ravimetric Method26
		sostatic Method27
_		uasi-Isostatic Method29
F.		rcial Permeability Test Systems
		<pre>xygen Transmission Rate Testers</pre>
		2) MAS 500 Oxygen Diffusion System33
		ater Transmission Rate Testers
		1) MOCON Permeatran WVTR Testers33
		2) MAS 1000 Moisture Permeation System36
	3. M	OCON Permatran C-IV CO <sub>2</sub> Permeability
		Testers36
		romatran Organic Vapor Permeability Testers38
	(4.	1) MOCON Aromatran Organic Vapor Permeation
		Series
	(4.	2) MAS 2000 Organic Vapor Permeability Test System41
		System
		S AND METHODS
A.	Materi	als For Synthesis of Clay/Polyimide
_		composites43
в.	Penetr	ants for Permeability Tests44
C.	syntne	sis of Clay/Polyimide Nanocomposite Film45
	1. P	reparation of Organically Modified  Montmorillonite45
		MODICHOLITIONICE43

<ol> <li>Preparation of 7% Polyamic Acid Solution45</li> <li>Preparation of Clay/Polyimide Composite Films46</li> </ol>
D. Permeability Test Methods and Equipment47
1. MOCON Permatran-W WVTR Tester48
2. MOCON Permatran-IV CO <sub>2</sub> Permeability Tester49
3. MOCON Ox-Tran 200 Permeability Tester50
4. MOCON Aromatran-1A Organic Vapor Permeability
Tester
(4.1) The Test Gas Delivery System and the Partial
Pressure of the Organic Vapor53 (4.2) Calibration Method55
(4.2) Calibration Method
(4.5) Test Parameters
RESULTS AND DISCUSSION
A. The Permeability Properties of Small Molecular Penetrans58
1. The Effect of Clay Loading on Water Vapor Permeation58
2. Oxygen Permeation
(2.1) The Effect of Clay Loading on Oxygen
Permeation
(2.2) The Effect of Temperature on the Oxygen
Permeability Coefficients63
3. The Effect of Clay Loading on CO <sub>2</sub> Permeation through
Clay/Polyimide Composites65
4. The Estimation of the Aspect Ratio of the Clay
Fillers67
5. Discussion72
(5.1) Comparison of the Barrier Properties of
Clay/Polyimide Nanocomposites to Literature
Values for Polyimides
Enhancement of Clay/Polyimide Nanocomposite
Films
1 111113
B. Organic Vapor Permeability Properties of Clay/Polyimide
Nanocomposite Films
1. Permeability of Polyimide Films with and
without Clay Inclusion77
2. The Effect of Test Temperature on the Ethyl Acetate
Permeability of Clay/Polyimide Nanocomposites79
3. The Effect of Ethyl AcetateVapor Pressure on the
Permeability of Polyimide Films with and without
Clay Inclusion
4. The Effect of Relative Humidity on the Permeability
of Ethyl Acetate through Polyimide Films with and without Clay Inclusion91
5. Estimation of Diffusion Coefficient Values for
Ethyl Acetate through Polyimide and 2.5%(v/v)
Clay Polyimide Films
can a caramance a aamoutition to the tree
ERROR ANALYSIS99

SUMMARY AND CONCLUSION	103
APPENDIX	
Appendix A: The Estimation of Diffusion Coefficient Values	106
Appendix B: Conversion Between SI Units and ASTM Units	108
BIBLIOGRAPHY	109

# LIST OF TABLES

Table 1 - Clay Loading and $H_2O$ Permeability Coefficient5 Table 2 - Clay Loading and $O_2$ Permeability Coefficient6
Table 3 - Effect of Temperature on Oxygen Permeability Coefficients of Clay/Polyimide Films64
Table 4 - Clay Loading and CO <sub>2</sub> Permeability Coefficient65
Table 5.1 - Relative Permeability of Clay/Polyimide to Water Vapor68
Table 5.2 - Relative Permeability of Clay/Polyimide to CO268
Table 5.3 - Relative Permeability of Clay/Polyimide to O <sub>2</sub>
Table 6 - Comparison of the H <sub>2</sub> O, O <sub>2</sub> and CO <sub>2</sub> Permeabilty Results with Literature Data
Table 7 - Ethyl Acetate Permeability Coefficients for 0% and 2.5% Clay/Polyimide Composite Films79
Table 8 - Ethyl Acetate Permeability Values Reported in the Literature for Selected Commodity Polymer Films
Table 9 - The Effect of Temperature on the Permeabilty of Ethyl Acetate through Clay/Polyimide Films80
Table 10 - Values of 1/T and Ln P for Ethyl Acetate Permeability83
Table 11 - Activation Energy Values for the Permeation of Ethyl Acetate through Polymer Films Reported in Literature85
Table 12 - Effect of Ethyl Acetate Vapor Pressure on the Permeability of Clay/Polyimide Composite Films86
Table 13 - Activation Energies at Different Vapor

	Pressures	90
Table	14 - Effect of Relative Humidity on Ethyl Acetate Permeability of Clay/Polyimide Films	93
Table	15.1 - Diffusion Coefficients for 0% Clay/Polyimide Films	96
Table	15.2 - Diffusion Coefficients for 2.5%(v/v) Clay/Polyimide nanocomposite Films	96
Table	16 - Comparison of the Diffusion of Ethyl Acetate at Low Vapor Activities in Polymers	97

## LIST OF FIGURES

Figure	<pre>1 - Structure Difference in Conventional Composite,     Intercalated and Exfoliated Clay/Polymer     Nanocomposites</pre>
Figure	2 - Water Vapor Permeability of Clay/Polyimide Nanocomposite Films as a Function of Clay Loadings
Figure	3 - O <sub>2</sub> Permeability of Clay/Polyimide Nanocomposite Films as a Function of Clay Loadings61
Figure	4 - Arrennius Plot of O <sub>2</sub> Permeabilty through Clay/Polyimide Composite62
Figure	5 - CO <sub>2</sub> Permeability of Clay/Polyimide Nanocomposite Films as a Function of Clay Loadings66
Figure	6.1 - Pc/Pp (H <sub>2</sub> O) vs. Clay Loading (v/v%)69
Figure	6.2 - Pc/Pp (CO <sub>2</sub> ) vs. Clay Loading (Vol%)70
Figure	6.3 - Pc/Pp (O <sub>2</sub> ) vs. Clay Loading (Vol%)71
Figure	7 - A Model for the Path of a Diffusion Gas Through the Clay Polyimide Hybrid74
Figure	8 - Transmission Rate Profile Plots for Polyimide and Clay/Polyimide Films
Figure	9 - Ethyl Acetate Transmission Rate Profile Curves for Polyimide Films Samples as a Function of Temperature81
Figure	10 - Ethyl Acetate Transmission Rate Profile Curves for Clay/Polyimide Films Samples as a Function of Temperature82
Figure	11 - Ethyl Acetate Permeability and Temperature Relationship84

Figure	12	- The Effect of Organic Vapor Pressure and Temperature on the Permeability of 0% Clay/Polyimide Film87
Figure	13	- The Effect of Organic Vapor Pressure and Temperature on the Permeability of 2.5%v/v Clay/Polyimide Film88
Figure	14	- Arrhenius Plot of Ethyl Acetate Permeability as a Function of Clay Loading and Permeant Partial Pressure89
Figure	15	- The Effect of Relative Humidity on the Permeabilty of Ethyl Acetate through Polyimide Films with and without Clay Inclusion92

#### INTRODUCTION

It has been proposed that a central problem to be solved by packaging engineers in the next century will be cost reduction (Packaging World Staff, PackExpo 96). Indeed, over the last decade, numerous efforts have been made by packaging professionals to reduce costs in the packaging industries. The most significant change, with respect to the selection of packaging materials, is the growing use of plastics, which occupies 35.1% of the market share of packaging materials (Boins, 1994). The trend for plastics to replace older packaging materials ensures a vigorous demand for plastic packaging in many sectors, well into the next century. addition to economy, modern plastics brings many other benifits to packaging, such as flexibility, light weight and multiple functionality. On the other hand, with the development of high-tech industries, such as microelectronics and space technology, packaging proposes new requirements for modern plastics. Users expect new packaging materials with high strength, light weight, high barrier, more functionality, and low cost. Furthermore, environmental concerns also require new packaging materials to meet source reduction requirements and to be recyclable (Rattray, 1994).

One of the answers to the above demands is clay/polymer nanocomposites. Due to their specific molecular textures, nanocomposites usually exhibit significant enhancement in mechanical, optical, conductive, nonlinear optical and barrier properties, as compared to the single components and conventional composites (Lan, 1994c).

Among various required properties, barrier properties are especially important to polymeric materials used in the packaging industry. In order to improve the barrier properties of polymeric materials, various procedures have been developed, to include: (I) co-polymerization, (II) crosslinking, (III) metallizing, (IV) laminating (Ford, 1995), (V) biaxially orientation, (VI) blending (Watanabe, 1987.), and (VII) SiOx coating (Felts, 1993.) (Brody, 1993). Normally, as barrier properties are increased, other properties of the polymer may also be altered.

Clay/polymer nanocomposites are a promising class of materials with potential applications in packaging.

Clay/polymer nanocomposites are usually stable after the hybrid complexes are formed, and do not undergo phase seperation. It can be produced in various forms, such as films and bulk materials, without additional supporting materials. In evaluating nanocomposites, because the reinforcement from the organic layers will occur in two rather than in one dimension, their mechanical properties are potentially superior to the respective component materials or even conventional fiber reinforced polymers (Krishnamoorti,

1996). In addition, the clay is dispersed to its molecular layer level in the polymer matrix, so the barrier efficiency of the clay is raised to its upper limit, which makes clay/polymer nanocomposites a unique barrier material.

When nanocomposites are used as a packaging material, the composite enhanced strength and barrier properties make it possible to produce packages with a lower amount of material, which is one way to achieve source reduction.

Also, clay resources abound in nature, and are cheap in cost. Thus, the incorporation of low loading level of clay can greatly improve the barrier properties of a polymer, and a significant cost reduction can also be realized.

Furthermore, when using a nanocomposite barrier material, the barrier properties are increased without requiring a multipolymer layered design, allowing for recycling. Thus, the clay/polymer nanocomposite is not only a low cost, high performance material, but also is an environmentally friendly material, which can lead to a new era of modern packaging materials.

In industry, it is now of great interest to develop technologies for processing clay/polymer nanocomposites.

According to the newest report (AMCOL web page, 1996), the AMCOL International Corporation has announced that its newest venture is in the field of nanocomposite technologies. The Corporation is positioned to capitalize on a proprietary technology that disperses nanoscale particles of chemically-modified clays into plastic resins, thus improving the

polymer's strength, heat stability and barrier properties.

Nanocor, Inc., a wholly owned subsidiary of AMCOL

International Corp. (NASDAQ:ACOL), is conducting an intensive feasibility study on locating its first commercial-scale production facility in Aberdeen, Miss. The company currently operates a pilot plant in Georgia, and expects to commercialize its technology during the course of 1997.

Targeted applications being considered range from flexible and rigid barrier packaging to structural components for trucks and automobiles (Nanocor web page, 1996). Some successful clay/polymer nanocomposite systems with packaging applications include polyethylene terephthalate (PET), polypropylene (PP), and ethylene-vinyl alcohol copolymer(EVOH), which involved the use of extruders (Lan, 1996).

In the present study, a clay/polyimide nanocomposite system was selected for investigation, and a comprehensive study was conducted to characterize the barrier properties of the composite. A polyimide structure was selected because polyimides may have packaging applications such as in electronics packaging, where barrier properties are of great importance. Secondly, it is possible to produce films of this kind of nanocomposite in laboratory conditions. The preparation of film of this kind of nanocomposite material has been successfully achieved by Lan (1994c).

To provide a better understanding of the barrier properties of the clay-polyimide nanocomposite, mass

dioxide, water vapor, and ethyl acetate vapor. The selection of the first three permeants is based on the fact that the permeability of these permeants are of primary concern when a polymer is used as a barrier material. Ethyl acetate was selected based on its common use as a solvent in the converting industry, and its presence as a residual from laminating and printing processes (Huang, 1996). Factors affecting the barrier properties of clay/polyimide nanocomposites including the clay loading, the test temperature, the organic vapor pressure and the relative humidity was evaluated. The conclusions of this study are not limited to this particular composite material but can be extended to other commodity polymer packaging materials. The specific objectives of this study include:

- 1. The preparation of clay/polyimide films composite containing 0-7.4%(v/v) CH<sub>3</sub>(CH<sub>2</sub>)<sub>17</sub>NH<sub>3</sub> montmorillonite clay.
- 2. Determine the permeability of the resultant clay/polyimide composites to oxygen, CO<sub>2</sub> and water vapor as a function of clay loading. The effect of temperature on the oxygen permeability will also be evaluated.
- 3. The evaluation of the effect of clay inclusion, the effect of temperature, ethyl acetate vapor partial pressure, and relative humidity on the permeability of clay/polyimide

and relative humidity on the permeability of clay/polyimide films to ethyl acetate vapor. The estimation of diffusion coefficients.

#### LITERATURE REVIEW

## A. Clay/Polymer Nanocomposites

1. Concepts of Composite and Nanocomposite Materials

A composite is a material which contains two or more component materials, which often has properties superior to each component. These superior properties come from the combination of the desirable characters of the individual materials. Composites have existed in nature for millions of years. Some well-known examples are wood, bones and shells of living creatures. With the development of synthetic polymer and fibers in composite systems, it is now possible to duplicate the structural advantages of natural materials, which has resulted in the manufacture and application of the high strength, light weight composites (Seferis, 1986).

Generally, there are several distinct phases in a composite. The continuous phase is called the matrix, and the discontinuous phase is called the filler. According to their structures, composites can be classified as metal/metal, metal/ceramic, ceramic/ceramic, ceramic/ polymer, and polymer/polymer composites (Lan, 1994c). Conventional composites are composed of fillers of the size of microns and up.

A nanocomposite is a type of material containing platelets that have at least one dimension in the size range of a nanometer, 1 billionth of a meter, or 1/25 millionth of an inch. Bentonite clay is one of the few materials that can be separated into platelets of a nanometer scale (Nanocor, 1996). The tiny size of the fillers makes the nanocomposite macroscopically homogeneous. So, the physical and mechanical properties of a nanocomposite are determined not only by the bulk properties of each component, but also by complex interactions between the building blocks and their interfaces. Nanocomposites usually exhibit a significant enhancement in mechanical, optical, conductive, nonlinear optical and barrier properties over the single component and conventional composites (Lan, 1994c).

Nanocomposites can be devided into two general categories, i.e. (I) intercalated nanocomposites and (II) exfoliated nanocomposites. Fig 1. shows the structural difference between conventional composites, intercalated and exfoliated nanocomposites. In conventional clay/polymer composites, which have been used for a number of years, mechanically crushed clays are mixed with polymer matrices. Clay tactoids exist in their original aggregated state and act only as fillers. These clay components simply save on polymer cost and play no functional role in determining the performance properties of the final composites. In an intercalated nanocomposite, organic polymer layers and inorganic silicate layers are alternatively interstratified

at the molecular level. In an exfoliated nanocomposite, the individual 10 Å-thick clay layers are dispersed in a continuous polymer matrix (Lan, 1994c). The average distances depend on clay loading.

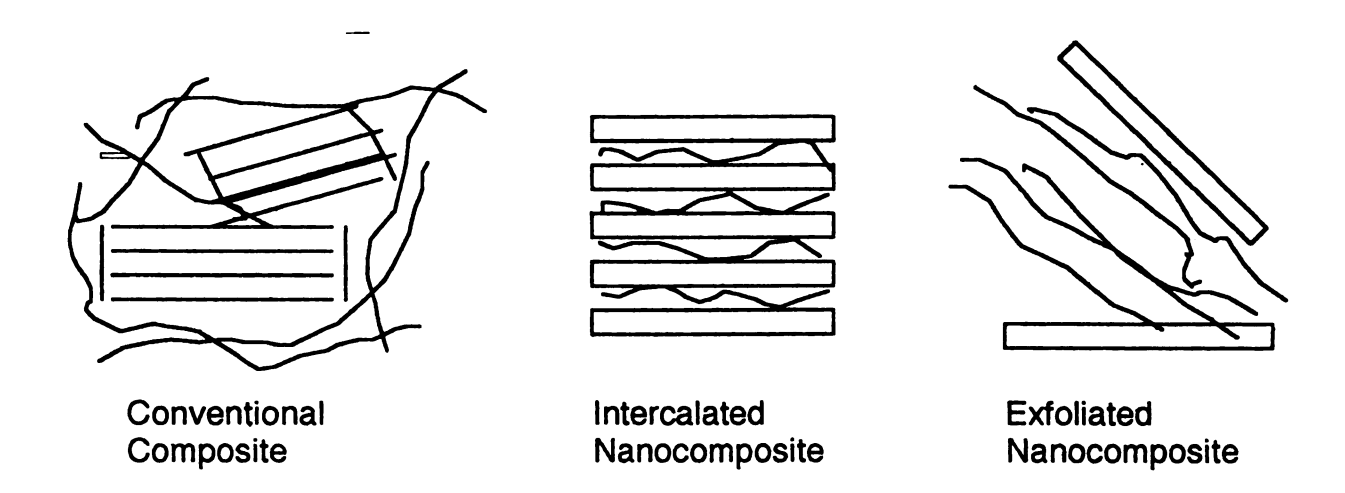


Figure 1. Structural Differences in Conventional, Intercalated and Exfoliated Clay/Polymer Composite/Nanocomposites (Lan, 1994c)

## 2. Recent Approaches in Clay/Polymer NanocompositeS

Although research on clay/organic polymer complexes has been carried on since 1965 (Blumstein, 1965; Lagaly and Beneke, 1975; Pinnavaia, 1983), world wide interest in this area was not realized until 1987, when Toyota researchers developed several nanoscale polymer-clay hybrid composites. These included systems based on the dispersion of an ω-amino acid and alkylammonium exchanged forms of montomorilonite clay in semicrystalline nylon-6 (Fukushima and Inagaki, 1987), (Fukushima et al., 1988), (Usuki et al., 1995b), amorphous epoxy (Usuki et al., 1989.), and polyimide (Yano et al., 1993; Lan and Pinnavaia, 1994a). The resultant

composites exhibited properties which were far superior to those of the pure polymer, or of conventional composite materials. The Toyota researchers reported that the clay/nylon-6 nanocomposites exhibited mechanical and thermal properties which were remarkably superior to those of the individual components. At a loading of 5.0 wt.% exfoliated clay, the tensile strength of the composite increased by 50% and the heat distortion temperature increased from 65 °C to 152 ℃ (Fukushima, 1987). These properties could not be duplicated by conventional organic chemical modification of the polymer. Transmission Electron Microscopy studies revealed that the improved performance observed was due to the formation of the nanoscopic composite. nanocomposites immediately found their use in the automobile industry, as the structural material of bumpers (Okada, et al., 1990). According to a recent report (Usuki, 1995b), nylon 6-clay hybrid materials containing four different types of clay minerals, montmorillonite, sponite, hectrite, and synthetic mica were compared. It was found that the nylon 6clay hybrid using montmorillonite, was superior to the other hybrids in mechanical properties. That was attributed to the montmorillonite clayinteracting strongly with nylon 6 by ionic interaction.

The intercalated clay/polymer nanocomposites are of interest because organic polymer layers and inorganic silicate layers are alternatively interstratified at the molecular level. Two synthetic approaches have been reported

to prepare intercalated clay/polymer nanocomposites. first is preformed-polymer-intercalation. The preformed polymer and clays are dissolved and dispersed in a solvent, respectively, then mixed. Upon solvent removal, a clay/polymer intercalated nanocomposite forms. Water soluble polymers, such as polyethylene oxide (PEO)(Ruiz-Hitzky, 1993), ethylene-vinyl alcohol copolymer (EVOH) (Tohoh, 1992) and polyvinyl alcohol (PVA)(Greenland, 1963) have been intercalated into clay galleries by this approach. Molten polymer can also be intercalated upon mixing with clays, such as polystyrene into organo-montmorillonite clays (Vaia et al., 1993). Limitations of this method are lack of convenient solvents for some polymers and the high viscosity of some molten polymers. The second method is the "in situ" intercalative polymerization method. The desired monomers are adsorbed or intercalated into the clay galleries. Then, the intercalated monomers are polymerized inside the clay galleries to form the clay/polymer nanocomposite. This method has been used extensively and overcomes the disadvantages of the first method. Various clay/polymer intercalated nanocomposites have been prepared by using the second approach. These include polyamide (nylon-6)(Kato et al., 1979), polymethyl metharcylate (Blumstein, 1965), polyaniline (Mehrotra and Giannelis, 1990), poly(ε-caprolactone) (Messersmith and Giannelis, 1993), polyacrylonitrile (Blumstein, 1974), and polyfurfuryl alcohol (Bandosz, 1992).

These intercalated nanocomposites have exhibited interesting electrical and optical properties.

At present, there are three major research groups world wide which are focusing on clay/polymer nanocomposites, these include Giannelis' group at Cornell University and Pinnavaia's group at Michigan State University in the United States, and the Toyota group in Japan. The most successful nanocomposites are those which showed enhanced mechanical and thermal mechanical properties, including those prepared with poly(ε-caprolactone) (Messersmith et al., 1993), epoxy resins (Lan and Pinnavaia, 1994b; Messersmith et al., 1994), polyimide (Lan and Pinnavaia, 1994a) (Giannelis, 1992), and polystyrene (Vaia et al., 1993). In addition, some reports showed that organoclay/polymer nanocomposites not only exhibited improved mechanical properties, but also showed ' improved barrier properties (Yano et al., 1993; Lan and Pinnavaia, 1994; Messersmith et al., 1995; Maul, 1995). For example, Messersmith and Giannelis (1995) studied the barrier properties of poly(ε-caprolactone) -layered silicate nanocomposites, and found that the water vapor permeability of nanocomposites containing as low as 4.8% silicate by volume, was reduced by nearly an order of magnitude as compared to pure poly(&-caprolactone).

Based on these finding, it is now of great interest to the industry to develop clay/nanocomposites processing technologies, as well. For example, Nanocor, Inc. was established by the AMCOL International Corporation,

specifically to develop clay-based technologies and products for the plastics industry (Nanocor web page, 1996). company claims that their unique, chemically modified clays, when added to plastic polymers form nanocomposites, an exciting new category of materials. Compared to the base polymer, a nanocomposite demonstrates improved heat resistance as well as enhanced structural and barrier properties. Nanocor has partnered with plastic resin producers and users to develop the special technologies and products suitable for several different polymer types. Targeted applications being considered range from flexible and rigid barrier packaging to structural components for trucks and automobiles. Pilot plant facilities have been established to advance process operations and produce trial quantities of NANOMER®, nano-sized platelets. Initial commercial production of some products is targeted for the second half of 1997. Nanocor received its first patent pertaining to the preparation of chemically modified clays and nanocomposites in September 1996, with others pending (Nanocor web page, 1996). Some successful polymer systems include PET, PP, and EVOH (Lan, 1996).

3. The Barrier Properties of Clay/Polyimide Nanocomposites
Polyimides are one of the most stable and
environmentally resistant polymer systems currently available
for use at temperatures up to 300 °C. They are marketed as
film, moldings and molding powders, wire coating enamels,

adhesives and laminating resins (Critchley and Wright, 1979). For example, Imi-Tech® Corporation manufactures a range of high performance, light weight, fire resistant SOLIMIDE® polyimide foam products for defense, industrial and commercial applications world wide. Those products are used as thermal and acoustical insulation in aerospace, marine and industrial markets, as well as for fire barriers, packaging and other applications requiring either high temperature or very low-temperature insulation in critical environments (Imi-Tech web site, 1996). Sykes and St.Clair (1986) studied the water vapor, oxygen and carbon dioxide transmission rates for a series of polyimides derived from either 3,3',4,4'benzophenone tetracarboxylic dianhydride (BTDA) or pyromellitic dianhydride (PMDA) with various diamines. et al.(1989) also studied the structure/ permeability relationships of nine different polyimides to H2, N2, O2, CH4, and CO<sub>2</sub>, with specific interest focused on application to the separation of gas mixtures.

Because of their heat resistance, chemical stability, and superior electric properties, polyimides are largely used for microelectronics and electronic packaging (Yano et al., 1993). But if they are used for advanced electronics, some properties are not sufficient. It is desired to reduce the amount of moisture absorption, the thermal expansion coefficient, and the dielectric constants of the polyimides. To improve these properties, many types of polyimides, having various chemical structures have been synthesized. One of the

examples included incorporating fluorine into the polymer backbone to reduce moisture absorption and dielectric constants for polyimides (Goff and Yuan, 1988; Labadie and Hedrick, 1990). However, these fluorinated polymers had poor mechanical properties. As a conventional method, clays are also used as fillers to obtain increased barrier properties (Muthy et al., 1986). Under such conditions, high levels of clay loading(40%) are needed, due to the low aspect ratios of the clay tactoids, which usually results in worsened mechanical properties.

As montmorillonite is composed of stacked silicate sheets, it has a low thermal expansion coefficient and high barrier properties. Therefore, if the clay/polyimide hybrid were synthesized, the above problems might be solved (Yano et al., 1993). The achievement of the synthesis of the clay/polymer nanocomposite led to a new and more efficient way to improve the barrier properties of polyimide. Due to their unique cation exchange properties, high aspect ratios of individual clay layers can be achieved (Lan, 1994c), thus only a small amount of organocation exchanged clay is needed to achieve increased barrier properties, as well as mechanical properties.

The earliest study on clay/polyimide nanocomposites, was carried out by the Toyota group (Fukushimaand and Inagaki, 1987, 1988; Yano et al., 1993). The Toyota researchers found that only 2 wt% addition of montmorillonite brought permeability coefficients of various gases to values less

than half of those of ordinary polyimide. Furthermore, the thermal expansion coefficients were reduced by 25% (Yano et al., 1993). It has been suggested that nearly complete dispersion (exfoliation) of the 10-Å-thick clay layer is needed to optimize the aspect ratio of the particles, which in the case of montmorillonite can reach a value of 200.

Recently, experiments at Michigan State University showed that similar composites, with an aspect ratio of 192, have enhanced CO<sub>2</sub> barrier properties (Lan and Pinnavaia, 1994a). Further, X-ray diffraction (XRD) results showed that the clay retained a crystallographically regular stacking order with a monolayer of polymer intercalated between the layers.

enhancement of clay/polyimide nanocomposites, Lan (1994c) compared the structural difference between exfoliated and intercalated clay/polyimide nanocomposites. In the exfoliated structure, the single 10-Å-thick clay layers act as filler elements. The aspect ratio of the individual plate and the filler loading determine the barrier property improvement. Whereas, in the intercalated structure, the clay fractal aggregates, and not single layers, function as filler elements (Lan, 1994c). The formation of the fractal clay structure for natural clay minerals is due to a water swelling effect. When the water molecules, which have been pre-intercalated into the clay galleries evaporate from the system, they tend to form a water domain region. This causes

the clay layers to slip and change their stacking pattern from turbostratic to a staircase fashion. For the polyamic acid and dimethylacetamide (DMAC) co-intercalated organoclays, the DMAC upon heating (100 °C) will leave the system. A rearrangement of the clay stacking then occurs to form the fractal structure of the clay in the polyamic acid matrix. After further heating at 300 °C, the clay fractal structure will remain simply because of the low mobility of the pre-formed polymer chains (Lan, 1994c).

While various researchers have proposed different mechanisms to account for the barrier property enhancement of clay/polyimide nanocomposites, the observed non-linear dependence of the permeability as a function of clay loading and the very low content of the inorganic phase, is crucial in developing light-weight composites.

### B. General Theory Rerlated to the Permeation Process

By definition, the permeability of a material is the flux or rate at which a quantity of penetrant passes through a unit surface area during unit time (Rogers, 1964).

There are several terms which have been used to describe the steady state permeation rate of molecules through a polymer film of surface area A and thickness 1 (Hernandez and Giacin, 1997).

• Permeant Transmisson Rate, 
$$F = \frac{q}{At}$$
 (1)

Permeance, 
$$R = \frac{q}{A \cdot t \cdot \Delta p}$$
 (2)

• Thickness Normalized Flow, 
$$N = \frac{q.1}{A.t}$$
 (3)

• Permeability Constant, 
$$P = \frac{q}{t} \frac{1}{A \Delta p}$$
 (4)

where q = the quantity permeated during time, t $\Delta p = p_2-p_1$ , pressure drop across the film

The permeation of a substance through a polymer is usually described by the permeability constant (or coefficient) P, which is a measure of the permeation rate of a gas or vapor through a polymer membrane at steady state. It is related to two fundmental parameters, D and S, by the expression:

$$P = D \times S \tag{5}$$

where D is the diffusion coefficient which is a kinetic term and describes how fast penetrant molecules move in a polymer host. S is a thermodynamic term called the solubility coefficient, which describes how many penetrant molecules dissolve in a polymer host. The above expression is valid when D is independent of permeant concentration and S follows Henry's Law of solubility.

According to the permeability model, a simple permeation process involves three basic steps: absorption, diffusion and

desorption. In the absorption step, penetrant molecules are absorbed and dissolved into the polymer surface which is exposed in a high penetrant concentration. In the diffusion step, the dissolved penetrant molecules then diffuse through the polymer membrane from the surface contacting the high penetrant concentration to the surface where the concentration is low. In the desorption step, penetrant molecules evaporate from the low concentration surface.

The sorption and desorption steps are related to the concentration of the penetrant in the polymer, and the penetrant vapor pressure in equilibrium with the polymer. The solubility of penetrants in polymers (especially polymers above their glass transition temperature and penetrants at low pressure) is described by the linear isotherm Henry's law of solubility:

$$c= S * p \tag{6}$$

where c is the concentration of gas in the polymer, p is the partial pressure of penetrant at the interface, and S is the Henry's law constant, which is the solubility coefficient. It can be assumed that the partial pressure of the penetrant is related to the penetrant concentration in the gas phase through the ideal gas law, when the concentration of the diffusant in the gas phase is very low (Hernandez et al., 1986).

The diffusion step is described by Fick's first and second laws of diffusion (Crank, 1975).

$$F = -D\left[\frac{\partial c}{\partial x}\right] \tag{7}$$

$$\frac{\partial c}{\partial t} = D \frac{\partial^2 c}{\partial^2 x} \tag{8}$$

where F is the flux or the rate of transfer of penetrant per unit area, c is the penetrant concentration in the polymer, x is the direction of the diffusion process, t is time, and D is the molecular diffusion coefficient.

Fick's first law is based on the hypothesis that the rate of transfer of a diffusing substance through a unit area of a section is proportional to the concentration gradient measured normal to the section. Fick's second law shows that the total change in the concentration across the slab bulk phase with time is directly proportional to the change in the concentration gradient with permeant penetration depth. The equation is valid in this form only if D is constant and the media is homogeneous. For most packaging applications, this is the case (Giacin, 1994). When the diffusion coefficient is independent of the penetrant concentration in the polymer, it is assumed that the diffusion process is Fickian. If the diffusion coefficient is a function of the penetrant concentration in the polymer, the diffusion process is said to be non-Fickian (Mears, 1965; Crank and Park, 1968).

# C. Factors Affecting the Permeability Properties of Polymers

There are several variables that can influence sorption, diffusion, and consequently the permeability coefficient.

They include the nature of the polymer, the nature of the penetrant, the penetrant concentration, temperature, and relative humidity.

First, the nature of the polymer, such as the polymer chemical composition, molecular structure and morphology can influence the solubility and diffusivity of a specific polymer/penetrant system. Typically, polymers with a high level of crystallinity, hydrogen bonding, high Tg, orientation, and low free volume, are likely to have low permeability rates. For instance, polyolefins appear to have good moisture barrier properties, since they are non-polar polymers and have a low affinity to moisture. On the other hand, polyamides (Nylons), polyvinylidienchloride (PVDC), and ethylene-vinyl alcohol copolymer (EVOH) offer high gas barrier properties, as well as solvent and odor barrier, because of their polarity and/or hydrogen bonding property (Dirienzo, 1993). Sykes and St. Clair (1986) studied the effect of molecular structure on the gas transmission rate of aromatic polyimides, and found that the molecular structure had a strong influence on the gas transmission rates obtained. The authors found that the barrier characteristics of the films investigated varied by three orders of magnitude for the respective polyimide films studied. In general, the 3,3',4,4'-benzophenone tetracarboxylic dianhydride (BTDA) series of polyimide film had overall, lower gas transmission rates than the pyromellitic dianhydride (PMDA) derived series. Polyimides prepared with meta-oriented diamines characteristically displayed lower gas transmission rates than those prepared with para-oriented diamines.

Secondly, the nature of the penetrant will affect the transport process. Small, non-polar and linear molecules, such as oxygen, helium, and carbon dioxide, have little interaction with polymer molecules, while permeating through the polymer matrix. Organic vapor molecules are large, have functional groups or have non-linear shapes, which makes the diffusion process more complicated. DeLassus (1993) reported that glassy polymers typicallyhave medium to high diffusion coefficients for oxygen and very low diffusion coefficients for flavor/aroma/solvent molecules at low concentrations.

Third, the temperature effect on permeability, diffusion, and solubility coefficients values can be described by the following Arrhenius relationship equations:

$$P(T) = P_0 \exp(-E_p/RT)$$
 (9)

$$D(T) = D_0 \exp(-E_D/RT)$$
 (10)

$$S(T) = S_0 \exp(DH_s/RT)$$
 (11)

where  $:E_p$  is the activation energy for permeation  $E_D$  is the activation energy for diffusion  $DH_s$  is the molar heat of sorption.

The above expressions are valid within a temperature range which does not include the polymer glass transition temperature. Usually, at temperatures above Tg, the permeability coefficient is more temperature dependent, while DeLassus below Tq, it is less temperature dependent. (1985) reported that an increase in temperature resulted in decreased solubility and increased diffusivity of limonene in oriented polypropylene. Huang (1996) studied the temperature dependent properties of the permeability coefficients of selected organic vapor penetrants through a series of barrier films, to include oriented polypropylene (OPP); saran coated oriented polypropylene (Saran coated OPP); high density polyethylene (HDPE); acrylic coated oriented polypropylene (Acrylic coated OPP); glassine; and a metallized polyethylene terephthalate (PET)/oriented polypropylene (Met PET/OPP) structure. The temperature dependency of the transport processes, over the temperature range studied, was found to follow well the Arrhenius relationship.

Relative humidity will also have a significant influence on hydrophilic polymers that are polar, or can form inter and intramolecular hydrogen bonding and a lesser affect on hydrophobic polymers such as polyolefins. For example, the permeability of ethyl acetate vapor through an ethylenevinyl alcohol copolymer (EVAL-F film) (Sajiki, 1991) was strongly affected by relative humidity. When the EVAL-F film was tested under dry conditions, there was little observed permeation. This can be attributed to the strong hydrogen

bonding between polymer chains, which restricts the diffusion of ethyl acetate vapor. When moisture is present, sorbed water plasticizes the hydrophilic barrier polymer which results in an increase in the permeation rate for ethyl acetate. On the other hand, Landois-Garza and Hotchikiss (1988) reported that an increase in relative humidity resulted in a decrease in the permeation of ethyl esters through polyvinyl alcohol (PVOH).

Other factors affecting permeation include: permeant concentration; plasticizers; and fillers. Concentration dependent effects have been observed on the permeability of organic compounds, such as aromas, flavors, and solvents by a number of investigators (Meares, 1965; Hernandez et al.,1986; Mohney et al., 1988). Some polymer systems (polyethylene and nylon 6) when filled with 40%wt of mica achieved a 60% decrease in H<sub>2</sub>O and O<sub>2</sub> permeabilities (Murthy et al., 1986). Recent studies on the permeability of nanocomposites showed that a significant enhancement in barrier properties was obtained with cation exchanged organoclays as fillers (Yano et al., 1993; Lan and Pinnavaia, 1994a).

## D. Models for the Permeability of Filled Polymers

Theories for the permeability of gases through polymers filled with inorganic powders are quite limited. Nielsen (1967) developed several simple models which show the trends

and limits to be expected for some of the effects of fillers on the barrier properties of the resultant composite. These models thus allowed interpretation of the observed experimental data. One model was developed to predict the maximum decrease in permeability that could be expected by the addition of a filler to a polymer.

When a polymer is filled with inorganic particles, it usually leads to a very tortuous pathway for molecules diffusing through it. In addition to the tortuosity factor, permeability rates are also reduced due to the fact that not all of a given cross section of material is pure polymer. As a first approximation, the following equation can be used (Nielsen, 1967):

$$P_F/P_u \approx \Phi_p / \tau$$
 (12)

where  $P_F$  and  $P_u$  are the permeabilities of the filled and unfilled polymer,  $\Phi_p$  is the volume fraction of the polymer, and  $\tau$  is the tortuosity factor. If it is assumed that the filler particles are circular or rectangular plates and that they are uniformly and completely dispersed in the polymer and that the plates are oriented parallel to the polymer film surface, it follows that:

$$\tau \approx 1 + (L / 2W)\Phi_{\rm F} \tag{13}$$

where L is the length of a face of a filler particle, W the thickness of the filler plates, and  $\Phi_F$  the volume fraction of filler. Combining Equation (12) and (13), the permeability equation becomes:

$$\frac{P_F}{P_W} = \frac{\Phi_p}{1 + (L/2W)\Phi_F}$$
 (14)

Equation (14) shows that thin plates with a large aspect ratio (L/W) can dramatically decrease the permeability of filled polymers, if the particles can be oriented so that their flat surfaces are parallel to the surfaces of the film.

### E. Permeability Measurement Methods

Permeability, diffusion and solubility coefficient values can be determined by the following procedures:

(1) Gravimetric Method:

In this procedure, permeation values are determined by observing the change in weight of a test cell or intact package system, as a result of the diffusion process. An example is the method described in ASTM E-96 (ASTM, 1988), where an aluminum dish containing desiccant is covered with a packaging material, weighed and placed in a constant temperature and humidity chamber. The samples are then weighed periodically, and the water vapor transmission rate is determined by the weight gain over time. Recently, an

electrobalance method has been used to measure the sorption and diffusion of organic vapors by polymeric meterials (Berens and Hopfenberg, 1982; Choy et al., 1984). The experiments are carried out at equilibrium vapor pressure, using an electrobalance which records continually the gain or loss of weight by a test specimen as a function of time. The gravimetric methods in general have low sensitivity, especially for high barrier polymer films, and are applicable over a limited vapor pressure range. However, application of the electrobalance negated these limitations and provide for high sensitivity and utility over a wide ranger of temperature and sorbate vapor pressure (Hernandez et al., 1986).

### (2) Isostatic Method:

In the isostatic procedure, a test film is clamped in a permeation cell which divides the cell into two chambers. A penetrant (test gas) flows continually through the high concentration cell chamber, and an inert carrier gas flows through the low concontration cell chamber. The partical pessure gradient of the penetrant, provides a driving force for the penetrant permeating through to the low concentration cell chamber, where the penetrant can be conveyed to a detector for quantification. Steady state is reached when the transmission rate, monitored continually, remains constant under constant conditions of temperature and permeant vapor pressure.

The permeability coefficient P is calculated from the transmission rate at steady state by the expression:

$$P = \frac{[C]_{\infty} \cdot f \cdot l}{A \Delta p}$$
 (15)

where  $[C]_{\infty}$  is steady state concentration of permeant conveyed to the detector, in mass per unit volume; f is the rate of carrier gas flow in the low concentration cell chamber, in volume per unit of time; l is the film thickness, in length unit; and A is the surface area, in area units. The diffusion coefficient D is determined by the following expression:

$$D = \frac{l^2}{7.199 \cdot t_{1/2}}$$
 (16)

where  $t_{1/2}$  is the time required to reach a transmission rate value that is equal to half of that at the steady state, in time unit.

Various detector devices have been used in isostatic permeability studies. Thermal conductivity detectors and thermistors were used to measure single permeants (Pasternak et al., 1970; Ziegel et al., 1969; Yasuda and Rosengren, 1970). Flame ionization detectors (FID) have been used for organic vapors and provide the advantage of not being affected by the presence of the carrier gas and water vapor (Zobel, 1982). When a complex mixture of organic permeants is involved in the test, a gas chromatograph was interfaced with an FID to separate individual permeant first before

performing quantification (Pye et al., 1976; DeLassus, 1985). Other techniques, based on either a photoionization detector or atmospheric pressure ionization mass spectrometer, were employed by Caldecourt and Tou et al.(1985). Both detection systems were found to be very sensitive and useful in the characterization of the prmeability of barrier membranes to organic penetrants. In some commercially available isostatic permeability testers, IR sensors and coulumetric sensors are also used for detecting water vapor and oxygen, respectively (MOCON, 1982; 1989).

### (3) Quasi-Isostatic Method:

The quasi-isostatic method is also called the accumulation method. In this procedure, diffusion and permeability coefficient values are obtained by quantifying the amount of the penetrant gas or vapor that has passed through the film and accumulated in the low concentration cell chamber, as a function of time. A test film is mounted betwen two cell chambers and the gas or vapor being tested is allowed to flow through the high concentration cell chamber. The partial pressure gradient provides the driving force for the penetrant permeating into the the low concentration cell chamber. Periodically gas samples in the low concentration chamber are removed and injected directly into a gas chromatograph (GC), where a flame ionization detector is used for quantification (Baner et al., 1986)

In this procedure, as the quantity of permeant accumulated in the low concentration cell chamber increases over time, the relationship between quantity accumulated per unit of time reaches a constant level, which means the permeation process has reached its steady-state status. The permeability coefficient can be determined from the flux at steady state and test constants (Hernandez et al., 1986). The permeability coefficient P is:

$$P = \frac{Q}{t \cdot A \Delta p}$$
 (17)

where Q is the total quantity of permeant that has penetrated during unit time (t). A is the test area exposed to the permeant, I is the film thickness and  $\Delta p$  is the driving force, expressed as concentration or partial pressure gradient. The duffusion coefficient (D) can also be determined by the lag time method, and is expressed as  $D = 1^2 / 6\theta$ , where  $\theta$  is the lag time and I is the film thickness. The lag time is obtained from the intersection of the projection of the steady state portion of the transmission curve to the time axis (Hernandez et al., 1986).

A number of investigators (Gilbert et al., 1983;
Hatzidimitriu et al, 1987; Mohney et al, 1988; Sajiki, 1993)
have studied the concentration dependence of the permeation
procedure, employing a quasi-isostatic system as described
above, which allows measurement of the permeation rate for
organic vapors at any desired low concentration level.

## F. Commercial Permeability Test Systems

Modern Controls, Inc. or MOCON (Minneapolis, MN) is a leading developer, manufacturer, and marketer of high technology instrumentation designed to test the barrier properties of packages and packaging materials. MOCON's testing instrumentation is used worldwide in research laboratories, production environments and quality control applications in the food, plastics, medical, and pharmaceutical industries (MOCON web page, 1996). MOCON permeability testers, which are commercially available, are designed for measuring gas, water vapor, and organic vapor permeability and are operatively friendly.

MAS Technologies, Inc. (Zumbrota, MN) is another manufacture of permeability instrumentation. Its products include the MAS 500 Isostatic Oxygen Diffusion System, the MAS 100 Moisture Permeation System and the MAS 2000 Organic Permeation Detector System.

The principle of both Modern Controls and MAS

Technologies' permeability instrumentation, is based on an
isostatic procedure. Typically, one film sample is mounted
between two cell chambers. One of the cell chambers holds
the test gas to be used as the permeant, while the other
chamber holds carrier gas that flows through the cell to the
detector. When the permeant diffuses from the high
concentration chamber into the low concentration chamber, it

is conveyed directly to the detector for quantitative measurement.

### 1. Oxygen Transmission Rate Testers

### (1.1) MOCON Ox-Tran Testers

At present, MOCON has developed several generations of Oxygen Transmission Rate Testers, including the Ox-Tran 100, Ox-Tran Twin, Ox- Tran 200, and Ox-Tran 2/20, which all meet the requirements of the ASTM D3985-81 Standard (ASTM, 1988).

Although the newer models are upgraded by using a computer and feature more functions, such as testing at relative humidity, the basic principle is the same, (i.e. an isostatic procedure). Also, the respective test systems all use the same detector type, which is a coulometric cell. The principle of which is based on well-known relationships established by Faraday (MOCON, 1989). It is a constant-current generator, the output of which is a linear function of the mass flow rate of oxygen entering the detector. In actual practice, the cell current is displayed in terms of the DC voltage developed across a fixed load resistance in the coulometric cell circuit. In the Ox-Tran 200 system, the use of a computer makes it possible to automatically select which resistor is to be used. Also, the use of a temperature control bath makes it convenient to test samples at subambient or elevated temperatures (5-50 ℃). Further, the newest generation, Ox-Tran 2/20 series have more functions and on advanced sensor system. MOCON engineers have developed a patented coulometric sensor (COULOX) with high performance, which provides parts-per-billion sensitivity even in the presence of water vapor (MOCON web page, 1996). There are three models of this kind of high performance sensor for testing films with different oxygen transmission rate range. The blue sensor is used for testing ultra-low range, the red sensor for mid-range, and the green one for ultra-high range. In addition to the advanced sensor, the 2/20 series provides the possibility for testing over a range of relative humidity conditions.

# (1.2) MAS 500™ Oxygen Diffusion System

The MAS 500<sup>TM</sup> Oxygen Diffusion System is designed to measure the precise levels of oxygen diffusion and solubility in packaging materials. The system incorporates precise temperature, RH, and flow rate control, a broad sensitivity range, high speed pentium-based computer control, and a software application package. System benifits include unmatched test throughput, solubility estimates for oxygen scalping and gas flush applications, automated test sequencing, and a full range of application analysis including oxygen desorption, absorption, and transmittance.

## 2. Water Vapor Transmission Rate Testers

### (2.1) MOCON Permatran WVTR Testers

The earliest standard test technique for measuring water vapor transmission rates, was classified as a "gravimetric"

test, and was based on the weight gain or loss over a period of time. This proceure met the requirements of the standard ASTM E-96. In practice, this method showed to be labor intensive, time consuming, and notoriously inaccurate (Demorest, 1995). In 1990, a new test standard, ASTM F1249-90, was adopted. This procedure is based on the isostatic method, and combines solid state electronics with a pulse-modulated infrared (PMIR) sensor, to detect down to one ppm of water vapor. During the test, when water vapor permeates through the film from the humidified side to the dry side, the density and the pressure of the carrier gas varies, and the absorption rate of infrared energy by water vapor also changes. The infrared photodetector and an amplifier senses the change in infrared energy, producing a DC output which is directly proportional to the water vapor in the exhaust of the test cell, and thus proportional to the water vapor transmission of the barrier material. The MOCON Permatran-W WVTR Tester, which was manufactured in the early 1980's, meets the requirement of this standard. In this method, the driving force was generated by placing saturated salt solutions on the humidified side. These salt solutions tended to corrode the test equipment, were messy and very operator dependent.

By later 1992, the Two-Pressure method of generating RH had been developed, which enabled the operator to create the desired relative humidity simply by adjusting the test gas pressure as it passes over a distilled water humidifier. In

this case, salt solutions were no longer necessary. The Two-Pressure method (MOCON, 1996) is based on the principle that if pure water and a pressurized gas are confined in a chamber, the gas will reach a relative humidity equilibrium of 100%. If that gas is released to an area (or another chamber) at a different (lower) pressure, the percent relative humidity in the new are will be reduced. The amount of reduction will be a ratio of the first and second pressures. For example, if the gas pressure within the humidifier is 29.4 psi and at 100% relative humidity, and is released to an ambient pressure of 14.7 psi (at sea level), its relative humidity will be 50%. The following formula can be used to determine RH at a given pressure:

 $100 - [psi_{Gauge} / (psi_{Gauge} + 14.7)] \times 100 = RH$ Where psi = pounds per square inch.

This method has been applied to the newest designed Permatran-W 3/31 WVTR Tester, as well as the Ox-Tran 2/20, the Permatran C-4/40, and the Aromatran 1A, which can measure gas or vapor permeabilities over a range of relative humidity conditions. The sensor for detecting the RH is one of the most advanced and reliable solid-state CMOS semiconductor device, which exhibits excellent stability and repeatability (MOCON, 1996). The Permatran-3/31 features a series of technological enhancements over prior models. It is faster and more stable, with increased upper and lower ranges, and 100 times greater sensitivity. It can perform tests directly

at the materials "real world" temperature and relative humidity (MOCON web page, 1996).

# (2.2) MAS 1000™ Moisture Permeation System

The MAS 1000™ Moisture Permeation System, designed by MAS Technologies, is another commercially available system for testing the levels at which moisture will permeate. Diffuse and solubility coefficient values for the packaging material can also be determined. It employs mass transport theory within a unique software package, which allows for early prediction of steady state permeation values. highly sophisticated system incorporated precise temperature and flow rate control, sensitivity in the 0.001 grams/m2/day region, and a high speed 486DX computer with a very accommodating software package. The test RH level is fully controlled through software to assure consistent and realistic measurements without the requirements of salt solution preparation. MAS 1000™ also incorporates a multiple zone cell to provide the user with significant improvement in test flexibility. This allows the user to select the appropriate test sensitivity level. Measurements requiring a high sensitivity may employ all zones while low sensitivity measurements may be conducted using a single zone.

## 3. CO<sub>2</sub> Permeation Testers

The most commonly used instrumentation for determining the permeability of CO2 includes the Permatran C-IV, Permatran-C200, and the newest model the Permatran C-4/40 designed by MOCON. These systems are based on the isostatic method, and use an infrared sensor with a closed loop system to circulate the trapped carrier gas. For the Permatran C-W, there are three methods which can be applied. The Static Accumulation method is used for testing low transmitting barriers, the Dynamic Accumulation method is used to measure moderate barrier structures having transmission rates generally greater than 50 cc/m<sup>2</sup>/day. The Continuous Flow method is a fast method to test barriers with moderate-tohigh transmission rates. The Permatran-C200 is interfaced to an IBM compatible PC, so all the test functions are well computer controlled. The system can test not only flat barrier films, but also packages, such as filled carbonated beverage containers. The PERMATRAN-C 4/40 unit performs tests directly at "real world" temperature and CO2 levels (MOCON web page, 1996). The system's transmission rate software will control up to 20 test cells in a system. In addition, the software reduces the possibility of errors with its ability to automatically determine equilibrium and compensate for any flow changes. Pre-programmed test formats, computer, and menu-driven screens make it easy to generate and interpret test data. Like all MOCON permeation test systems, the PERMATRAN-C 4/40 is modular. A flexible, dual film test cell configuration and optional Package

Environmental Chamber allows for testing both flat films and finished packages.

# 4. Organic Vapor Permeation Test Systems

Although studies on organic vapor permeation by isostatic and quasi-isostatic test procedures have been carried on for a period of time, there is no test standard for such studies, since the measurement of organic vapor permeation is quite complicated. Research workers usually designed their own systems to conduct organic permeation studies. The various procedures developed for quantifying the rate of diffusion of organic penetrants through polymeric membranes have been described by Hernandez, et al. (1986). In responce to the industries demand for a convenient instrumental system, MAS Technologies (Zumbrota, MN) first developed, the TMI MAS 2000<sup>TM</sup> Organic Permeation test system in 1994. In 1995, MOCON announced its competitive products, Aromatran Series, i.e. Model 1A and Model 2.

### (4.1) MOCON Aromatran Organic Vapor Permeation Series

The Aromatran 1A is a fully modular and automated system designed to test single permeants under dry or at specified relative humidity conditions, with a test temperature range from 5 °C to 65 °C. The Aromatran Model 2 is an effective and semiautomatic means of testing multiple permeants. The builtin cryotrap also provides increased sensitivity for high barrier materials.

The Aromatran series are also based on Fick's first and second laws and Henry's law. The test results provide permeability, diffusivity and solubility coefficient values for test films, where the relationship of these three values is  $P = S \times D$ . Here, the assumption that the film permeability follows Fickian behavior, is a prerequisite condition for this system. The test system directly measures the permeability of the film to organic vapor by utilizing a calibrated FID detector. The approach of finding the diffusion coefficient D when P is known, is the "half time" method, which requires finding the time  $(t_{1/2})$  at half the final permeation rate. When using  $t_{1/2}$ , we can get D from the following equation:

$$D = \frac{l^2}{7.199 \cdot t_{1/2}} \tag{16}$$

where l is the thickness of the film. When P and D are known, S can be found by using S = P/D.

The half-time method requires the film to be outgassed first, so the film is void of the permeant. Then the film is challenged with a permeant on one side and the other side is swept with a carrier gas to keep the permeant concentration at zero. The technique involved here is called the void/differential (VD) method. Another technique which can be used is the Saturated/Differential (SD) method, which has been found to be the fastest and most common test today(MOCON, 1996). In the SD method, no outgassing is necessary, and the film is "saturated" with the permeant at

the start of the test. The SD method is applied only when permeability of the film structure is required. If the three respective permeability parameters are required, the VD method is the method of choice. The VD method is also applied to the prediction function that is provided by the Aromatran 1A.

The prediction method requires iteratives of an equation with two unknowns. It can be described as following (Pasternak et al., 1970):

$$\frac{F_{\infty}}{F_{t}} = \frac{4}{\sqrt{\pi}} \cdot \sqrt{\frac{1^{2}}{4Dt}} \cdot e^{-\frac{1^{2}}{4Dt}}$$
 (18)

Let 
$$x_1 = \frac{1^2}{4Dt_1}$$
 (19)

$$F_{\infty} = \frac{F_{t}}{\sqrt{\pi} \cdot \sqrt{x_{1}} \cdot e^{-x_{1}}}$$
 (20)

$$D = \frac{1^2}{4 x_1 t_1}$$
 (21)

$$S = \frac{F_{\alpha}}{D} \tag{22}$$

Fortunately, a value for x can be calculated for every value of time (t) and thus the diffusion coefficient D, the

solubility coefficient S and the permeability coefficient  $F_{\infty}$  (P) can be determined. One of the primary conditions of any method or equation used to determine the diffusion coefficient D, requires the permeant of interest to be sufficiently outgassed from the polymer before the polymer is challenged by the permeant. This is very important because most polymers have retained residual organic volatiles, which can be measured by the FID sensor.

# (4.2) MAS 2000 Organic Vapor Permeability Test System

The permeation theory of the MAS 2000 System is based on Fick's first and second laws, as well as Henry's Law. steady state permeability value, P, is assumed to be the product of the material's solubility coefficient, S, and the diffusion coefficient, D, as described by the expression  $P = D \times S$ . Based on the isostatic procedure, the apparatus allows for the continuous collection and measurement of the permeation rate of the organic vapor through a polymer film, from the initial time zero to steady state conditions (Huang, 1996). Interfaced to an IBM 486SX computer, the MAS 2000 system demonstrates good temperature and flow rate control, and it is convenient to perform on-sreen operations and mornitoring. For each test, one film sample can be placed in the diffusion cell. The test can be performed at dry conditions only, with a test temperature range from room temperature to 200 °C.

Recently, the MAS 2000 System was modified with a device for trapping permeated organic vapors employing a dynamic purge and trap technique (Chang, 1996), by MAS Technologies, Inc. in collaboration with the School of Packaging (Michigan State University, East Lansing, MI). In this modified configuration, the trapping system was designed to ensure that the sample cell chamber is continuously flushed with the carrier gas and the permeated vapor is conveyed to the trapping tube attached. The Dynamic Purge and Trap/Thermal Desorption Procedure Showed an increase in sensitivity of three to four orders of magnitude over the continuous flow isostatic procedure (Chang, 1996).

### MATERIALS AND METHODS

# A. Materials for Synthesis of Clay/Polyimide Nanocomposites

1. Natural montmorillonite

Source Clay Mineral Depository
University of Missouri, Columbia, Missouri
unit cell: Na<sub>0.86</sub>[Mg<sub>0.86</sub>Al<sub>5.14</sub>(Si<sub>8.00</sub>)O<sub>20</sub>(OH)<sub>4</sub>]

2. 4,4'-diaminodiphenylether (4,4'-ODA)

Aldrich Chemical Co. (Milwaukee, WI)

Molecular Weight: 200.24

Melting Point: 190-192 ℃

Purity: 99%

3. Pyromellitic dianhydride (PMDA)

Chriskev Company, Inc. (Leawood, KS)

Molecular Weight: 218.12

Melting Point: 286.7 ℃

Purity: 99%

4. Dimethylacetamide (DMAC)

Aldrich Chemical Co. (Milwaukee, WI)

Molecular Weight: 87.12

Melting Point: -20 ℃; Boiling Point: 164-166 ℃

Purity: 95%

5. Octadecylamine (18A)

Aldrich Chemical Co. (Milwaukee, WI)

M.W. 269.52

Melting Point: 55-57 ℃

Purity: 99%

## B. Penetrants For Permeability Tests

1. Oxygen

LIQUID CARBONIC Specialty Gas Co. (Chicago, IL)

Purity: 2% O<sub>2</sub>, 98% nitrogen balance

2. Carbon Dioxide

AGA Gas, Inc. (Cleaveland, OH)

Purity: 99.9%

3. Ammonium Phosphate Monobasic (For making saturation solution to generate 90%RH in the headspace)

Mallinckrodt Chemical Works (St. Louis, MO)

Purity: Analytical Reagent

# 4. Ethyl acetate (CH<sub>3</sub>COOC<sub>2</sub>H<sub>5</sub>)

J. T. Baker Chemical Co. (Phillipsburg, NJ)

Analytical Reagent grade

Molecular Weight: 88.11

Boiling Point: 77.2 +/- 0.5 ℃

purity: 99.9%

## C. Synthesis of Clay/Polyimide Nanocomposite Film

Clay/Polyimide nanocomposites film samples were prepared following the procedure and formular discribed by Lan (1994c).

# 1. Preparation of Organically Modified Montmorillonite

Organclays were synthesized by an ion exchange reaction (Lin, 1992) The cation exchange reaction was carried out by adding 2.0 g of montmorillonite to 500 ml of 0.05 M alkylammonium chloride ethanol:water (1:1) solution and the solution stirred at 70 °C for 24 hours. The exchanged clay was washed several times with ethanol:water (1:1), until no chloride ions was detected with a 1.0M AgNO $_3$  solution, and the clay then was dried. Dried clay samples were ground and the 40-50  $\mu$ m fraction was collected.

## 2. Preparation of 7% Polyamic Acid Solution.

Polyamic acid was synthesized by the condensation reaction between 4,4'-diaminodiphenylether (4,4'-ODA) and Pyromellitic dianhydride (PMDA) in Dimethylacetamide (DMAC). A stoichiometric amount of PMDA was slowly added to the 4,4'-ODA/DMAC solution with vigorous stirring at 15-20 °C. The mixture was then stirred an additional hour at room tempeature. The final polyamic acid solution has a concentration of approximately 7 wt%.

# 3. Preparation of Clay/Polyimide Composite Films

A known amount of clay powder (the amount depends on the desired clay loading in the resultant film) was added to a 20 gram solution of polyamic acid and the solution was stirred vigorously at room temperature for 24 hours, followed by 2

hours to settle. The solution was then poured onto a glass plate and dried at room temperature to form a self-supporting film. The air-dried polyamic acid-clay films were then heated at 2°C /min to 250°C and maintained at 250°C for 4 hours, to form cured polyimide-clay hybrid composites.

## D. Permeability Test Methods and Equipment

In this study, the MOCON Permatran-W WVTR Tester, the Permatran-IV CO<sub>2</sub> Permeability Tester, the Ox-Tran 200 Permeability Tester and the Aromatran 1A Permeability Tester were used. A general description of the test gas delivery

system, calibration method and test parameters is briefly summarized below for the respective test units.

#### 1. MOCON Permatran-W WVTR Tester

The Permatran-W WVTR Tester consists of two units, namely the measuring system and the sample conditioning system (MOCON, 1982). Usually, up to five film samples can be conditioned while the sixth one is being tested. Each test film is clamped in a diffusion cell, with one side of the film exposed to a continuous flow of dry air, the other side is exposed to water vapor from the moistened pad in the upstream cell cavity.

The carrier gas in the test chamber is connected to an infrared sensor, which monitors the moisture amount permeated through the film. The infrared response generates an electrical signal that can be read from a volt meter.

Calibration of the sensor is done with a PET standard film of known WVTR value, to determine the calibration factor. The specific calculation is:

The WVTR is given in unit of  $g/(m^2 \cdot day)$ .

In this study, each film sample was mounted in a masking device (Modern Controls, Inc) to reduce the test area, since the polyimide has a high water vapor transmission rate. The test parameters are:

Test temperature: 37.8 °C

Relative Humidity: 90%

Carrier gas flow: 150 cc/min

# 2. MOCON Permatran-IV CO<sub>2</sub> Permeability Tester

The Permatran C-IV is an instrument designed for measuring the rate at which gaseous carbon dioxide diffuses through a permeable barrier material, such as flat film, a plastic bottle, and other flexible packaging systems. The instrument incorporates a means for programmed operation in which each of the samples are tested automatically, in sequence, with minimum operator attention. Data are recorded by a strip chart recorder (MOCON, 1983).

When testing a flat barrier material, each film is clamped between the upper and lower halves of a diffusion cell. Gaseous carbon dioxide is admitted into the upper chamber, and pure nitrogen is flowed into the bottom chamber. The bottom chamber is connected to the infrared sensor and pump that creates a closed loop around which the trapped carrier gas is circulated. The infrared sensor monitors the increased CO<sub>2</sub> concentration in the carrier gas and generates an electronic signal. The CO<sub>2</sub> transmission rate is then derived from the slope of the trace recorded by the recorder.

Calibration of this instrument is accomplished routinely by injecting measured increments of  $CO_2$  into the volume being sensed and noting the voltage change produced.

In this study, due to the high CO<sub>2</sub> permeability of the polyimide films, each film sample was mounted in a masking device, which reduced the test area from 50 cm<sup>2</sup> to 5 cm<sup>2</sup>, so measurable results could be obtained. Some parameters used in the test include:

Carrier gas flow: 250 cc/min

CO<sub>2</sub> flow: 80 cc/min

Test temperature: 25 °C

## 3.MOCON Ox-Tran 200 Permeability Tester

The Ox-tran 200 is an extremely sensitive instrument designed to measure the rate at which dry or humidified  $O_2$  gas passes through a barrier material mounted in the test chambers of the diffusion cell. The system is computer-controlled and has several options including packaging testing. This system meets the requirements of ASTM D3985 (MOCON, 1989).

When operating with flat films, the test films are mounted in the diffusion cells, the test temperature and the flow rate of the gases are adjusted and the test parameters are entered into the computer. Upon initiating the run, the computer will commence testing the film specimens and

continue until the oxygen transmission rate reaches a constant value. At that time, the computer will terminate testing and store the data until printout.

Calibration of the Ox-tran 200 is carried out by testing a PET standard film of known  $O_2$  transmission rate value, then comparing the test value with the known value, and entering the ratio of those two values into the computer as Gas Sensor Gain. Any value of oxygen transmisson rate obtained from the measurement of the film being tested is then multiplied by the "gas senor gain" value. The Ox-Tran 200 reports values of the oxygen transmission rate, in units of  $cc/(m^2.day)$ .

In this study, to obtain measurable results, an aluminum foil masking device was used to reduce the film area exposed to the test gas. In addition, a gas cylinder with  $2\% O_2$  and  $98\% N_2$  balance was used as the test gas. In conducting the test, the following operating parameters were used: Carrier gas and test gas tank output: 30 psi

N<sub>2</sub> flow rate: 30 cc/min

Test gas flow rate: 20 cc/min

Conditioning time: 10 hours

Examination time: 10 min (It specifies the duration of an examination of any given cell for each cycle during the test process.)

Test temperature: 23 °C for evaluating the effect of clay loading; 0, 5, 15, 23, 30 °C for the effect of temperature.

4. MOCON Aromatran-1A Organic Vapor Permeability Tester The Aromatran-1A Permeability Tester is specifically designed for testing the permeation of aromas, flavors, odors, and solvents under dry or at a specified relative humidity. The two film test unit, incorporates an FID detector, and is interfaced to a pentium IBM compatible computer. The computer controls the entire test procedure, undertakes data collection, and the final results calculations. The build-in RH sensors, temperature controller, barometer and flow meter, which are controlled and monitored by the computer, make the testing system well controlled under desired conditions. Furthermore, the "generated RH" method (Demorest, 1995) is employed to generate the precise desired humidity, so it is possible to test samples at "real world" conditions. The final report provides not only the results of permeability, but also the values of diffusion and solubility for the tested penetrant/polymer system, at the test temperature and vapor partial pressure.

To test a flat film, the film sample is mounted in one of the test cells. Testing takes place entirely inside the test cell. The test temperature and humidity of the gases are selected, and the test parameters and other test information

required are entered into the computer. Once the test is initited, the computer tests the film as instructed. The computer will terminate testing and store the data until printout (MOCON, 1996).

(4.1) The Test Gas Delivery System and the Partial Pressure of Organic Vapor

The test gas delivered can be a certified gas or sparging gas. In this study, a sparging gas was used. The permeant to be studied is placed into the sparger, and a carrier gas is passed through the liquid in such a manner so as to obtain a known and stable concentration of the permeant in the test gas stream. The test gas stream is connected directly to the test gas input port of the Aromatran 1A. Test gas flows are normally set at 15 to 30 cc/min.

When the temperature controller bath is set at a specified temperature, the organic liquid inside the sparger generates a fixed and constant saturation vapor pressure at that specific temperature. It is suggested that the sparging system should be maintained at a temperature 15  $^{\circ}$ C below ambient to insure that there is no condensaton within the delivery system. In this study, the sparger was set at either 0  $^{\circ}$ C or -10  $^{\circ}$ C depending upon the desired vapor activity. The resultant organic vapor partial pressure in the test cell is equal to the the saturation vapor pressure

generated in the sparger. The conclusion is based on the following reasoning (Hernandez, 1996):

### Asssumptions:

(i) At points A and B, the mass flows are equal.

therefore,  $M_1=M_2=M$ , where M is the mass flow (mass/time) (ii) The organic vapor pressure is usually very low, and therefore the mass flow consists primary of air. For this case, it can therefore be assumed that the organic vapor behaves as an ideal gas.

therefore,  $F_2 = F_1 * T_2/T_1$ 

and by definition: c = M/F, where F is gas flow rate (volume/time)

So, the concentration,

at point A:  $c_1 = M_1/F_1$  and

at point B:  $c_2 = M_2/F_2$ 

Then,  $c_2/c_1 = T_1/T_2$ 

When expressing c or p by the ideal gas law, at point A: p = nRT/v = R/MW \* m/v \* T = R/MW \* c\* T  $P_2/p_1 = c_2*T_2/c_1*T_1$   $p_2 = p_1 *1/c_1*T_1 *c_1*T_1/T_2 * T_2 = p_1$ 

So, at point A and B:

- · Temperatures are different
- · Mass flows are equal
- · Flow rates are different
- · Partial pressures are equal

### (4.2) Calibration Method

The calibration of the Aromatran 1A is based on the two point method(Loebig,1996). In the Aromatran 1A, the relationship between the FID response and the organic vapor partical pressure is assumed to be linear between two points. Therefore, only one point needs to be obtained experimentally, since the second point is assumed to be zero. The specific operation includes introducing the test gas stream directly to the FID, and entering the information about the molecular weight of the permeant, and the partial pressure of the organic vapor to the computer. The calibration test is initiated when the system shows a stable baseline. This operation provides for determination of a relationship between detector output and vapor partial pressure. The relationship is computed and then stored in the

program memory. Following calibration, a permeability test can be initiated. Here, the transmission rate profile is monitored on the screen until a constant signal response is observed. The permeability parameters are then directly calculated by the software program.

# (4.3) Test Parameters

In this study, permeability tests were carried on at three temperatures, 15, 23, and 30 °C, respectively. At each temperature, two ethyl acetate vapor partial pressures were evaluated, i.e. 3205 Pa (24.36 mmHg) and 1693 Pa (12.87 mmHg). Other operation perameters include:

Gas tank outlet pressures:

 $N_2$  (as sparging gas): 4 psi (dry test); 18 psi (wet test)  $N_2$  (as carrier gas): 10 psi (dry test); 40 psi (wet test) Air: 50 psi

H<sub>2</sub>: 50 psi

Test gas flow = 15 cc/min

Carrier gas flow = 15 cc/min

Hydrogen flow = 4 cc/min

Air flow = 132 cc/min

FID temperature = 140 ℃

Sparger bath temperature:

O ∞ (for generating 24.36 mmHg ethyl acetate vapor pressure)

```
-10 °C (for 12.87 mmHg)
```

Exam Time (min) = 15 (for getting steady state permeability
values)

Rezero Frequency = 1 (for getting steady state permeability
values)

Individual Zero = No (for permeability values)

Cycle count = Infinite

Relative humidity = 0, or 50%

Film area =  $50 \text{ cm}^2$ 

#### RESULTS AND DISCUSSION

### A. The Permeability Properties OF Small Molecular Penetrants

### 1. The Effect of Clay Loading on Water Vapor Permeation

The permeability of clay/polyimide nanocomposite films to water vapor was determined with a MOCON Permatran-W WVTR Tester. The test conditions were 37.8 °C, 90%RH. During the test, an aluminum foil mask was used for each film to reduce the test area of the film samples, so the detector output values fell within a measurable range. The WVTR values

Table 1. Clay Loading and H2O Permeability Coefficient

Clay Loading	H <sub>2</sub> O Permeabilty Coefficient <sup>(a)</sup>		
(v/v%)	[g.mil/(m <sup>2</sup> .day.mmHg)] <sup>(b)</sup>	[10 <sup>-15</sup> kg.m/(m <sup>2</sup> .sec.Pa)]	
0	8.62 ± 0.21	19 ± 0.5	
1.25	4.06 ± 0.34	9.1 ± 0.8	
2.5	3.43 ± 0.27	7.6 ± 0.6	
5.0	2.43 ± 0.13	5.4 ± 0.3	
7.5	1.45 ± 0.10	3.2 ± 0.2	

- (a) Average of replicate analyses
- (b) Permeability coefficient expressed in ASTM standard units
- (c) Permeability coefficient expressed in SI units

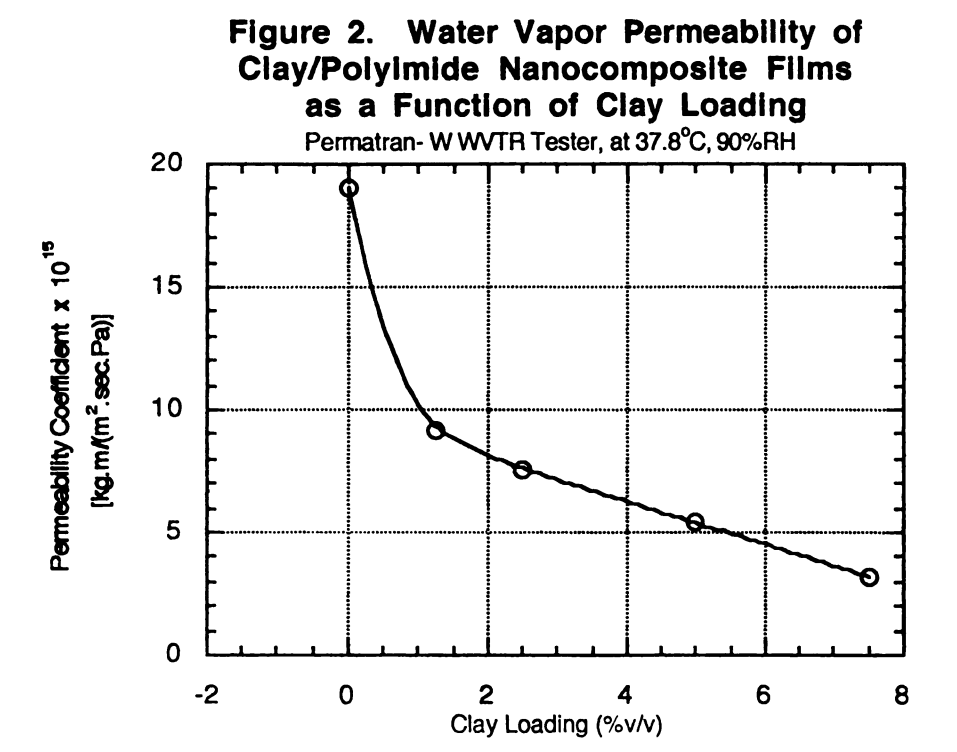
obtained were converted into permeability coefficients to describe the moisture barrier characteristics of the test films. Table 1 summarizes the effect of clay loading on the water vapor permeability coefficients of the respective clay/polyimide films. Each value is the average of replicate runs and is expressed in both ASTM and SI units. The results are also presented graphically in Figure 2, where the permeability coefficient is plotted as a function of clay loading.

As shown, compared with a pure polyimide film, the clay /polyimide hybrid composites exhibited a significant reduction in water vapor permeability. Further, there is a non-linear dependence of  $H_2O$  permeability, as a function of clay loading. For example, the addition of only 1.25%(v/v) clay resulted in approximately a 50% reduction in the permeability coefficient, as compared to the permeability coefficient of the pure polyimide.

#### 2. Oxygen Permeation

(2.1) Permeability Coefficients of Oxygen Through Clay/polyimide Films as a Function of Clay Loadings

The oxygen transmission rate studies were carried out on an Ox-Tran 200 Oxygen Transmission Rate Tester. In order to get measurable results, not only was a aluminum foil mask used to reduce the sample surface area, but the upstream oxygen concentration used was 2% (v/v), rather than the standard pure oxygen or a 21% oxygen mixture. The  $O_2$ 



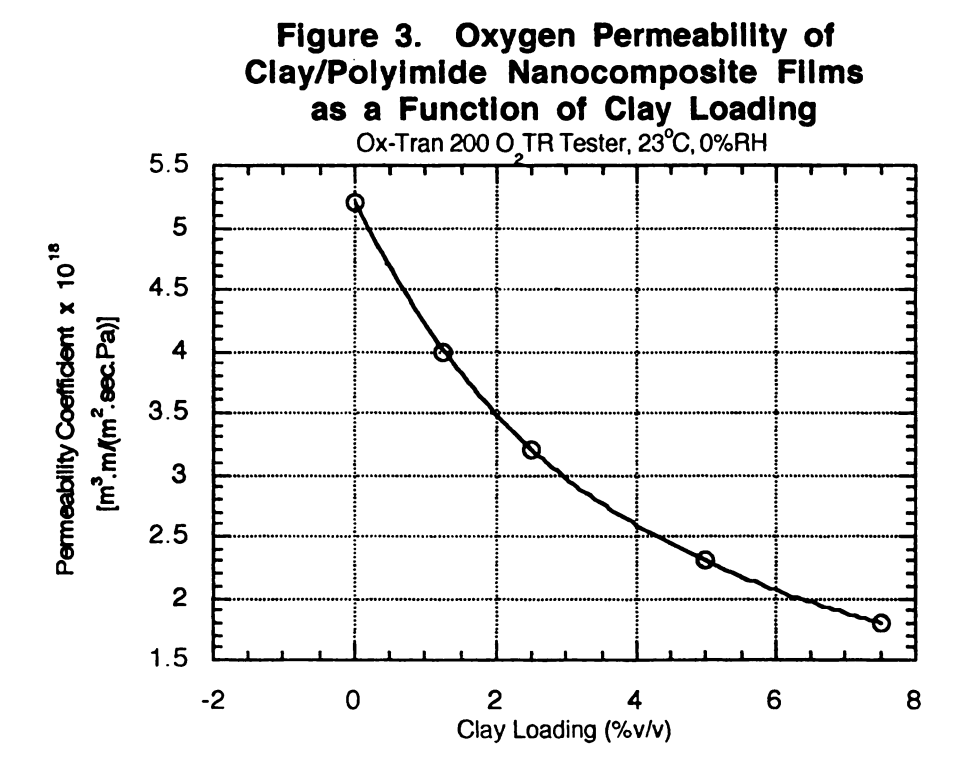
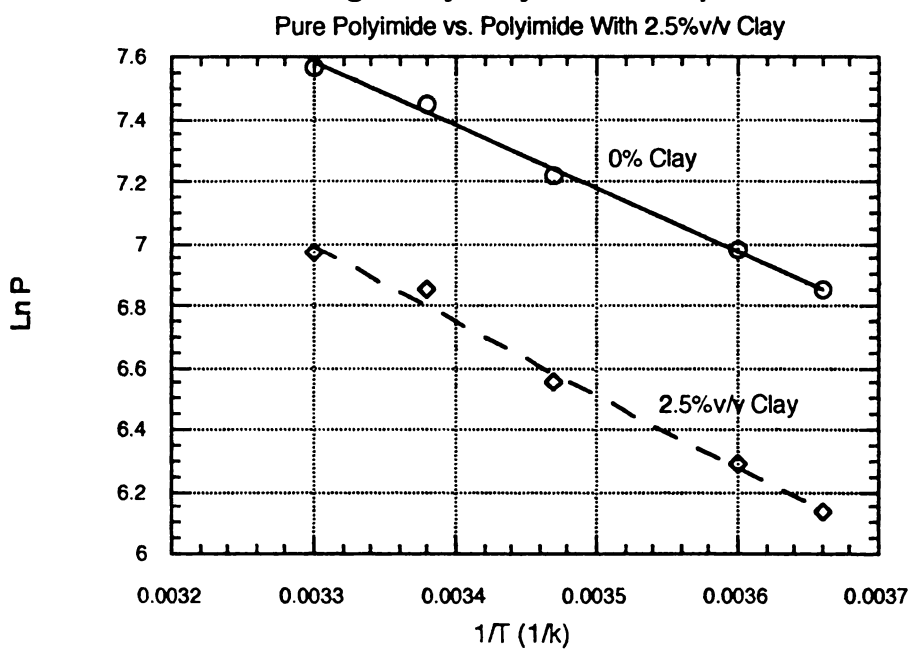


Figure 4. Arrhenius Plot of O<sub>2</sub> Permeability
Through Clay/Polyimide Composite



permeability coefficient values for the polyimide films with various clay loading levels are summarized in Table 2, and are expressed in both ASTM and SI units. To provide a better understanding of the effect of clay loading on the barrier characteristics of the clay/polyimide nanocomposite films, the permeability coefficient values are also plotted as a function of clay loading (see Figure 3).

As shown, the incorporation of clay into the polyimide hybrid resulted in a significant reduction in oxygen permeability, with a 50% reduction in the O<sub>2</sub> permeability coefficient achieved at a 2.5% clay loading level.

Table 2. Clay Loading and O<sub>2</sub> Permeability Coefficient

Clay Loading	O <sub>2</sub> Permeability Coefficient <sup>(a)</sup>		
(v/v%)	<pre>[cc.mil/(m<sup>2</sup>.day.atm)]<sup>(b)</sup></pre>	[10 <sup>-18</sup> m <sup>3</sup> .m/(m <sup>2</sup> .sec.Pa)]	
0	2321 ± 552	6.8 ± 1.6	
1.25	1353 ± 133	4.0 ± 0.4	
2.5	1082 ± 139	3.2 ± 0.4	
5.0	791 ± 23	2.3 ± 0.1	
7.5	601 ± 20	1.8 ± 0.1	

- (a) Average of replicate runs
- (b) Permeability coefficient expressed in ASTM standard units
- (c) Permeability coefficient expressd in SI units

### (2.2) The Effect of Temperature on the Oxygea Permeability Coefficients

The temperature dependency for  $O_2$  permeability, over the temperature range 0-30 °C, was also determined for the clay/polyimide hybrids. Table 3. summarizes the results

obtained for the pure polyimide film and the polyimide film with 2.5%v/v clay loading. Values are the average of replicate runs and are reported in both ASTM and SI units.

From Table 3, it becomes evident that the permeability coefficient exhibits a temperature dependence at a constant

Table 3. Effect of Temperature on Oxygen Permeability Coefficients of Clay/Polyimide Films

Temperature (°C)	Permeability Coefficient(a) [cc.mil/(m².day.atm)](b)		Coeffic [10 <sup>-18</sup> m <sup>3</sup> .m/	ability cient <sup>(a)</sup> (m <sup>2</sup> .sec.Pa)]
	Clay Loading		Clay I	oading
	0%v/v	2.5%v/v	0%v/v	2.5%v/v
0	942	463	2.75	1.36
5	1074	540	3.16	1.59
15	1371	703	4.03	2.07
23	1724	943	5.07	2.77
30	1934	1059	5.69	3.11

- (a) Average of replicate runs
- (b) Permeability coefficient expressed in ASTM standard units
- (c) permeability coefficient expressed in SI units

permeant concentration level. This is illustrated in Figure 4, where the permeability coefficient is plotted as a function of temperature [1/T (°K-1)], for the studies carried out. As can be seen, the temperature dependency of the transport process, over the temperature range studied (0-30 °C), follows well the Arrhenius relatioship. From the slopes of the Arrhenius plots, the activation energy for the permeation process (Ea) was determined for the respective film samples and the following values obtained:

0% clay/polyimide: Ea = 16.8 KJol/mole (4.038 KCal/mole)
2.5%(v/v) clay/polyimide composite: Ea = 19.6 KJol/mole
(4.692 KCal/mole)

The Arrhenius expression used to describe the permeability coefficient as a function of temperature is typically applied over a temperature range above or below the glass transition temperature  $(T_g)$  of the polymer, but not within a temperature range which includes  $T_g$ . A straight line extrapolation typically cannot be made through  $T_g$  and graphical analysis is expected to show a change in slope at the  $T_g$ . This was assumed not to be a concern for the polyimide based structures, since the  $T_g$  of the polyimide  $(T_g = 399 \, ^{\circ}\text{C})(\text{Sykes}, 1986)$  is well above the maximum temperature evaluated in the present study.

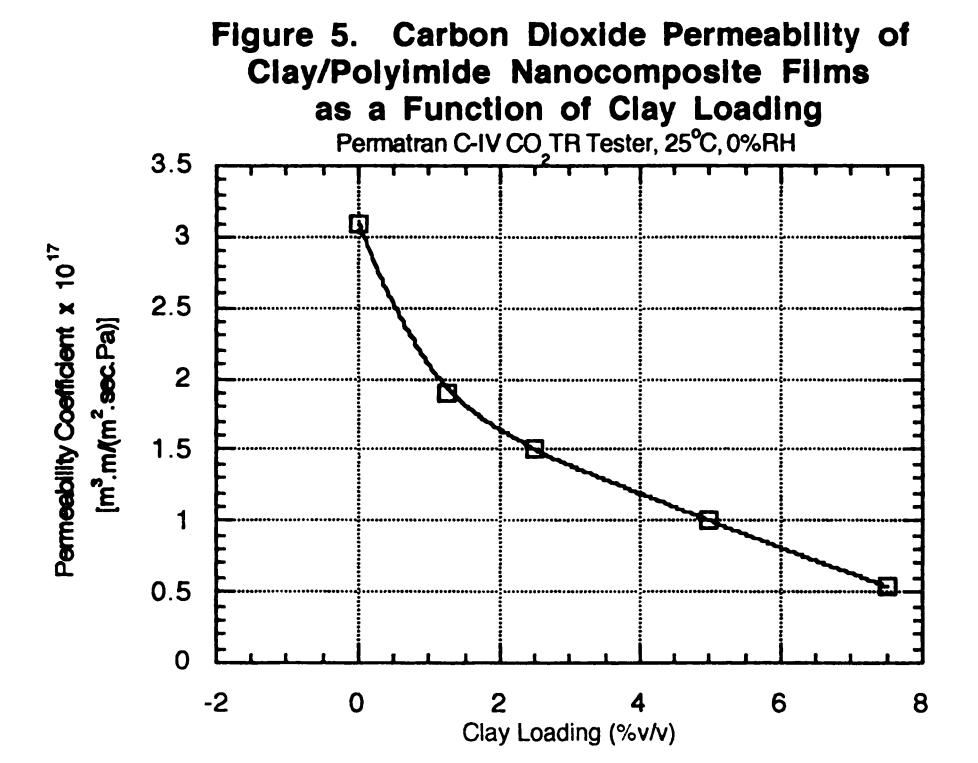
# 3. The Effect of Clay Loading on Carbon Dioxide Permeation through Clay/Polyimide Composites

Table 4. Clay Loading and CO2 Permeability Coefficient

Clay Loading	Permeability Coefficient(a)		
(v/v%)	[cc. mil/( $m^2$ .day.atm)] [ $10^{-17}$ m <sup>3</sup> .m/( $m^2$ .sec		
0	10516 (b)	3.1 (b)	
1.25	6519 ± 24	1.9 ± 0.01	
2.5	5154 ± 983	1.5 ± 0.3	
5.0	3812 ± 132	1.1 ± 0.03	
7.5	1852 ± 257	0.54 ± 0.08	

<sup>(</sup>a) Average of replicate runs

<sup>(</sup>b) No measurable deviation from mean was calculated for replicate runs



The  $CO_2$  transmission rate studies were carried out on the Permatran C-IV  $CO_2$  Permeability Tester. The permeability coefficient values calculated are summarized in Table 4. Figure 5 shows graphically the relationship between  $CO_2$  permeability coefficient and the clay loading level.

From the results presented above, it appears that there is a non-linear dependence of  $CO_2$  permeability, as a function of clay loading, with the addition of 2.5%(v/v) clay resulting in a 50% reduction in the  $CO_2$  permeability coefficient. This is supported by the results of Lan (1994c), who studied the permeation of  $CO_2$  through clay/polyimide nanocomposite films and reported that there was a nonlinear dependence of  $CO_2$  permeability on clay loading for a series of composite films containing 0-7.4% montmorillonite clay.

#### 4. The Estimation of the Aspect Ratio Of Clay Fillers

According to Nielsen(1967), the dependence of permeability on filler (i.e. clay)loading can be estimated from the equation:

$$\frac{P_F}{P_U} = \frac{\Phi_p}{1 + (L/2W)\Phi_F}$$
 (14)

where  $P_F$  and  $P_U$  are the permeability values for the composite film and that of the unfilled control film, respectively.  $\Phi_P$  and  $\Phi_F$  are the volume fractions of polymer and filler, and L/W is the width-to-thickness ratio, or the aspect ratio, of the filler. Based on this expression, the aspect ratio can be

estimated from relative permeability data ( $P_F/P_U$ ). Tables 5.1, 5.2 and 5.3 summarize the relative permeability data for

Table 5.1. Relative Permeability of Clay/Polyimide to Water Vapor

Clay Loading	Relative Permeability
(v/v8)	$(P_F/P_U)$
0	1
1.25	0.47
2.5	0.39
5.0	0.28
7.5	0.17

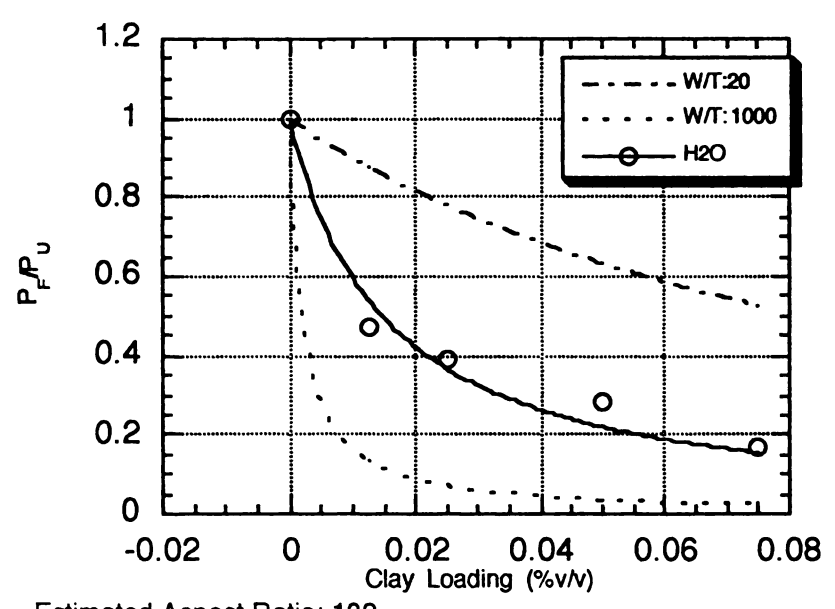
Table 5.2. Relative Permeabilty of Clay/Polyimide to CO2

Clay Loading	Relative Permeability
(v/v%)	$(P_F/P_U)$
0	1
1.25	0.62
2.5	0.54
5.0	0.36
7.5	0.18

Table 5.3. Relative Permeability of Clay/Polyimide to O2

Clay Loading	Relative Permeability
(v/v%)	$(P_F/P_U)$
0	1
1.25	0.58
2.5	0.47
5.0	0.32
7.5	0.26

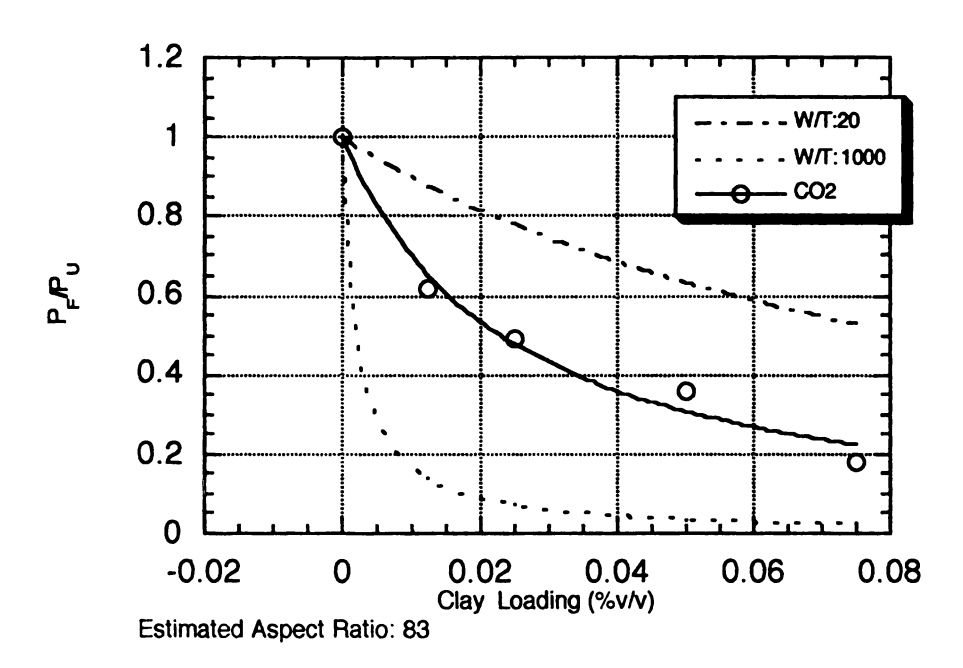
Figure 6.1.  $P_F/P_U$  ( $H_2O$ ) vs. Clay Loading (v/v%)



Estimated Aspect Ratio: 132

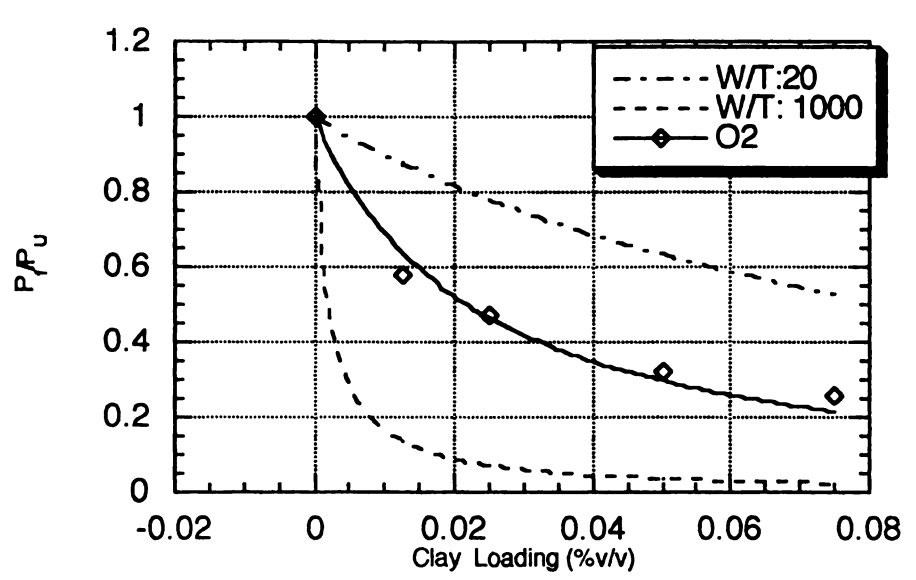
y = (1-m0)/(1+(m1/2)*m0)		
	Value	Error
m1	132.39	16.035
Chisq	0.0092412	NA
R	0.98875	NA

Figure 6.2.  $P_F/P_U$  (CO<sub>2</sub>) vs. Clay Loading (v/v%)



y = (1-m0)/(1+(m1/2)*m0)		
	Value	Error
m1	83.426	7.3816
Chisq	0.0056643	NA
R	0.99256	NA

Figure 6.3.  $P_F/P_U$  (O<sub>2</sub>) vs. Clay Loading (v/v%)



Estimated Aspect Ratio: 87

y = (1-m0)/(1+(m1/2)*m0)		
	Value	Error
m1	87.684	7.9146
Chisq	0.0058398	NA
R	0.99147	NA

water vapor, CO2 and oxygen, respectively. Figures 6.1, 6.2 and 6.3 present graphically the results obtained by application of equation 14 and the experimental data. The solid curve represents the best fit of the calculated values from equation 14 to the experimental data. The dashed curves are calculated for fillers with aspect ratios of 20 and 1000, which are representatives of nonintercalated and completely exfoliated clay particals, respectively. The best fit curve yields an apparent clay aspect ratio of approximately 132 from the water vapor relative permeability data, 83 when using the CO2 relative permeability data, and an aspect ratio of 87 from the O2 relative permeability data.

#### 5. Discussion

# (5.1) Comparison of the Barrier Properties of Clay/Polyimide Nanocomposite to Literature Values for Polyimides

Sykes and St. Clair (1986) determined the water vapor, oxygen and carbon dioxide barrier properties for a series of polyimides. Table 6. summarizes both the permeability coefficient values of the polyimide based samples evaluated in this study and the values reported by Sykes and St. Clair (1986). The polyimide films in both studies were synthesized from the same materials. Data are reported in both ASTM and SI units.

As shown in Table 6, the results obtained in this study were in good agreement with the literature values, for the

simple polyimide samples. This indicates that the films prepared in the present study were of good quality (i.e. level of pinholes, uniform thickness) and the permeability values determined were representative of the polyimide structure.

Table 6. Comparison of the  $H_2O$ ,  $O_2$ ,  $CO_2$  Permeability Results with Literature Data

	Permeability Coefficient		
	Literature <sup>(a)</sup> This study		
	Polyimide	0% Clay Polyimide	2.5% Clay Polyimide
PH2O at 37.8℃			
kg.m/(m².sec.Pa) <sup>(b)</sup>	1.6 x 10 <sup>-14</sup>	1.9x 10 <sup>-14</sup>	0.76 x10 <sup>-14</sup>
g.mil/(m <sup>2</sup> .day.mmHg) <sup>(c)</sup>	6.94	8.62	3.43
PCO2 at 23 °C			
$m^3 \cdot m/(m^2 \cdot sec \cdot Pa)^{(b)}$	4.0 x 10 <sup>-17</sup>	3.1 x 10 <sup>-17</sup>	$1.5 \times 10^{-17}$
cc.mil/(m <sup>2</sup> .day.atm) <sup>(c)</sup>	13651	10516	5154
<b>PO2</b> at 23 °C			
$m^3.m/(m^2.sec.Pa)^{(b)}$	1.2 x 10 <sup>-17</sup>	0.68 x10 <sup>-17</sup>	0.32 x 10 <sup>-17</sup>
cc.mil/(m <sup>2</sup> .day.atm) <sup>(c)</sup>	3975	2321	1082

- (a) Data are converted from original Transmission Rate value (Sykes & St. Clair, 1986)
- (b) Permeability coefficient expresed in SI units
- (c) Permeability coefficient expressed in ASTM standard units

## (5.2) The Interpretation of the Barrier Property Enhancement of Clay/Polyimide Nanocomposite Films

Permeation studies showed that for  $O_2$ ,  $CO_2$  and water vapor as penetrants, the incorporation of low loading levels of clay (i.e. 2.5 %v/v) dramatically reduced the permeability

The dramatic lowering of the of polvimide films. permeability characteristics of the nanocomposites is attributed to the presence of dispersed, large aspect ratio, clay layers in the polymer matrix. Previous work (Bissot, 1989) on the barrier properties of polymer films containing conventional clay-type fillers showed that a large amount of clay loading (40%wt) is required to reduce the permeability of the clay filled structure, owing primarily to the low aspect ratio (less than 20) of the particles. The method used for preparing the film in the present study can result in, in-plane orientation of the clay layers, which are impermeable to penetrant molecules. This forces penetrant molecules permeating through the film to follow a tortuous path through the polymer matrix surrounding the clay particles, thereby increasing the effective path length for diffusion. Figure 7. shows such a model.

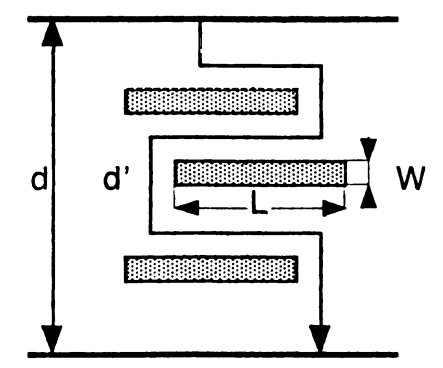


Figure 7. A Model for the Path of a Diffusing Gas Through the Clay/Polyimide Hybrid (Yano et al., 1993)

Previous studies on the montmorillonite clay/polyimide system, described by Yano et al.(1993), showed that the clay was dispersed homogeneously within the polyimide matrix and was oriented parallel to the film surface. So the total path of the diffusing gas was therefore increased. In this hybrid, the clay consisted of stacked silicate sheets about 2000 Å in length, 10 Å in thickness (Yano et al., 1993), to give an aspect ratio of 200.

The X-ray crystallography results descibed by Lan (1994c) for a montmorillonite clay/polyimide nanocomposite showed that the clay retained a crystallographically regular layer stacking order, with a monolayer of polymer intercalated between the layers. This is consistent with a possible self-similar clay aggregation mechanism, where the face-face associated layers are slipped in a staircase-like fashion. In order to more fully characterize the particle texture, Transmission Electron Microscope (TEM) images were obtained on thin sections of the clay-polyimide hybrid and two characteristic domains were observed. There were domains of highly exfoliated clay layers, as well as domains of regularly intercalated layers. The aspect ratio reported by Lan et al.(1994a) was 192.

The aspect ratio determined in the present study ranged from 132 to 83 and is within the range of 200 to 70, which was reported by Yano et al.(1993), Lan et al.(1994 a,c) and Messersmith et al.(1995). It was assumed that the clay texture in the nanocomposite films evaluated in the present

study would be similar to that obtained by Lan (1994c), since the chemistry and methodologies employed in both studies were similar. The aspect ratios reported in this study were estimated from the permeability data and the solution of Equation 14, and are therefore assumed to be a bulk property of the clay/polyimide hybrid with both exfoliated and intercalated domains contributing to the resultant permeability values. The exfoliated state of the clay was considered to be important to the barrier property of the composite films (Lan, 1994c). Also, it should be pointed out that the diffusion path model is based on the assumption that the impermeable clay layers are perfectly oriented and evenly spaced within the plane of the film, a situation not likely to be realized in actual composite film structures (Messersmith et al., 1995).

The observed enhancement in the barrier properties is of great importance in evaluating clay/polymer nanocomposites for use in packaging and other applications where efficient polymeric barriers are needed. For these applications, a significant reduction in permeability can result from either increased barrier efficiency, or reduced thickness of the barrier layer for the same efficiency (Messersmith et al., 1995).

### B. Organic Vapor Permeability Properties of Clay/Polyimide Nanocomposite Films

To develop a better understanding of the mass transfer properties of nanocomposites films, with particular emphasis on organic permeants, studies to determine the permeability of clay-polyimide nanaocomposite films to ethyl acetate were carried out with the MOCON Aromatran-1A Permeability Tester. This test system is based on an isostatic test procedure.

Permeability studies were carried out on polyimide film with 2.5%(v/v) clay loading and on film without clay added.

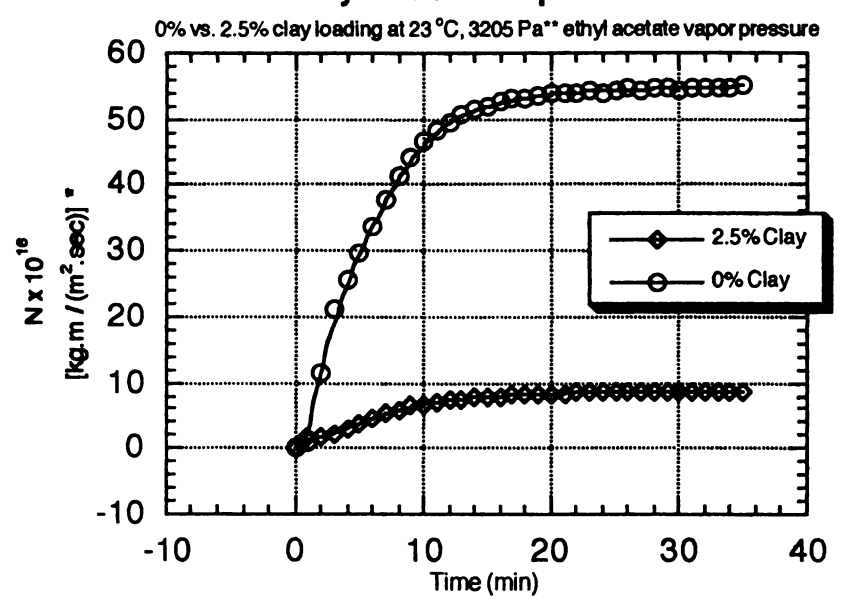
The effect of the temperature, organic vapor activity and relative humidity, on the barrier characteristics of the test polyimide films, was evaluated.

## 1. Permeability of Polyimide Films with and without Clay Inclusion

To evaluate the effect of clay loading on the barrier characteristics of the nanocomposite films, tests were carried out at constant tempeature (23 °C) and permeant vapor pressure ( $\Delta p = 3.2$  KPa). Replicate runs were carried out and the mean permeability coefficient values reported. The results are summarized in Table 7.

As shown in Table 7, there was an 85% reduction in the permeability coefficient for the clay/polyimide film, when compared to the polyimide film without clay loading. Fig 8. presents the transmission rate profile curves for the test polyimide films (i.e. with and without clay), and illustrates graphically the significant reduction in the transmission rate of the polyimide film with clay inclusion. Similar

Fig 8. Transmission Rate Profile Plots for Polyimide Composite Films



<sup>\*</sup> Normalized Transmission rate: Data are thickness normalized

<sup>\*\*</sup> Partial pressure of ethyl acetate in test gas

results were obtained for studies carried out at different test temperatures and organic vapor concentrations (see Table 9 and 12).

When the ethyl acetate permeability coefficient values were compared to these obtained for selected commodity films (see Table 8), it was found that polyimide films, and in particular the clay/polyimide composite films, had much better barrier properties to ethyl acetate.

Table 7. Ethyl Acetate Permeability Coefficients for 0% and

2.5%(v/v) Clay/Polyimide Composite Films

Clay Loading	No.	Permeability Coefficient x 10 <sup>18</sup> (a)(b)
(%v/v)		[kg.m/( m².sec.Pa)]
	1	1.22
0	2	1.27
	Avg.	1.24 ± 0.03
2.5	1	0.186
	2	0.189
	Avg.	0.188 ± 0.002

(a) Partial pressure of ethyl acetate = 3.2 KPa

(b) Temperature of test = 23 °C

Table 8. Ethyl Acetate Permeability Values Reported in the Literature for Selected Commodity Films

Polymer Structure	$P_{E.Ac}$ . x $10^{17}$ (kg.m/m <sup>2</sup> .sec.Pa)
Oriented Polypropylene	2.0 (a)
Glassine	5.7 (a)
High Density Polyethylene	40 (a)
0% Clay/Polyimide	0.12 (b)
2.5%(v/v) Clay/Polyimide	0.019 (b)

(a) Determined at 30 °C (Huang, 1996)

(b) Determined at 30 °C (This study)

### 2. The Effect of Test Temperature on the ethyl Acetate Permeability of Clay/Polyimide Nanocomposites

Both the pure polyimide and the 2.5%(v/v) clay/polyimide nanocomposite films were tested at 15°C, 23°C, and 30°C, respectively. Tests were performed at dry conditions, with a penetrant vapor partial pressure of 3.2 KPa (24.36 mmHg). The results are summarized in Table 9.

Table 9. The Effect of Temperature on the Permeability of Ethyl Acetate Through Clay/Polyimide Films

Temperature	No.	Permeability Coefficient x 10 <sup>18</sup>	
(℃)		[kg.m/(m <sup>2</sup> .sec.Pa)]	
		0% Clay/Polvimide	2.5%Clay/Polyimide
		Films	Films
1.5		1 10	0.170
15	+	1.19	0.178
	2	1.17	0.173
	Avg.	1.18 ± 0.01	0.175 ± 0.003
23	1	1.22	0.186
	2	1.27	0.189
	Avg.	1.24 ± 0.03	0.188 ± 0.002
30	1	1.34	0.189
	2	1.39	0.190
	Avg.	1.37 ± 0.03	0.190 ± 0.001

From the above results, it appears that the test temperature does not markedly affect the permeability of ethyl acetate through the polyimide and clay loaded polyimide films, over the temperature range studied. However, as shown, there is a slight increase in the permeation rates for both film structures as a function of temperature. Typical transmission rate profile curves, as a function of

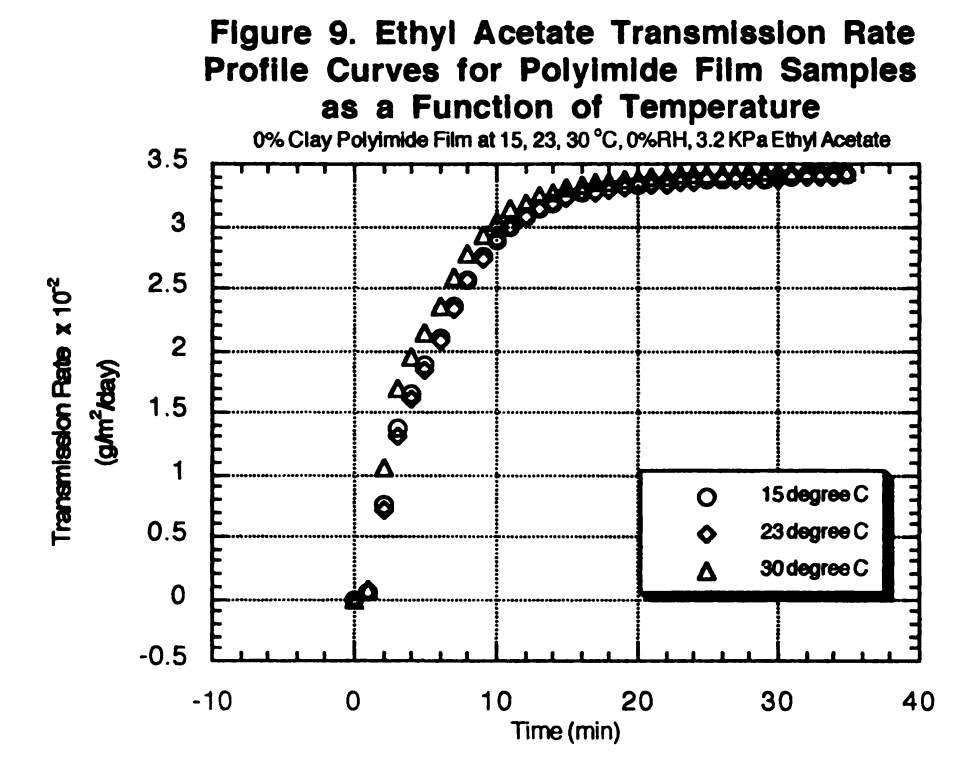


Figure 10. Ethyl Acetate Transmission Rate
Profile Curves for 2.5%v/v Clay/Polyimide
Film Samples as a Function of Temperature

3.5

2.5%v/v Clay/Polyimide Film at 15, 23, 30 °C, 0%RH, 3.2 KPa Ethyl Acetate

3.5

2.5

2

3

3

2.5

4

0

15degree C

23degree C

30degree C

Time (min)

-10

-0.5

temperature, for both test films are presented in Figures 9 and 10, respectively.

Table 10. summarizes the values of Ln P and 1/T, converted from the above data. The Arrhenius plot of the permeability data, where Ln P is plotted as a function of  $T^{-1}$  ( $K^{-1}$ ), is presented in Figure 11.

Table 10. Values of 1/T and Ln P for Ethyl Acetate Permeability

I OI MOUDILIE			
Temperature (oC)	1/T (°K <sup>-1</sup> )	Ln Pl (0% Clay)	Ln P2 (2.5% Clay)
15	0.003472	-41.281	-43.190
23	0.003378	-41.231	-43.118
30	0.0033	-41.132	-43.107

The relationship between Ln P and 1/T for both films is described by following expressions:

(1) 0% Clay polyimide

Ln P = 
$$-38.317-856.5/T$$
, R =  $0.97013$ 

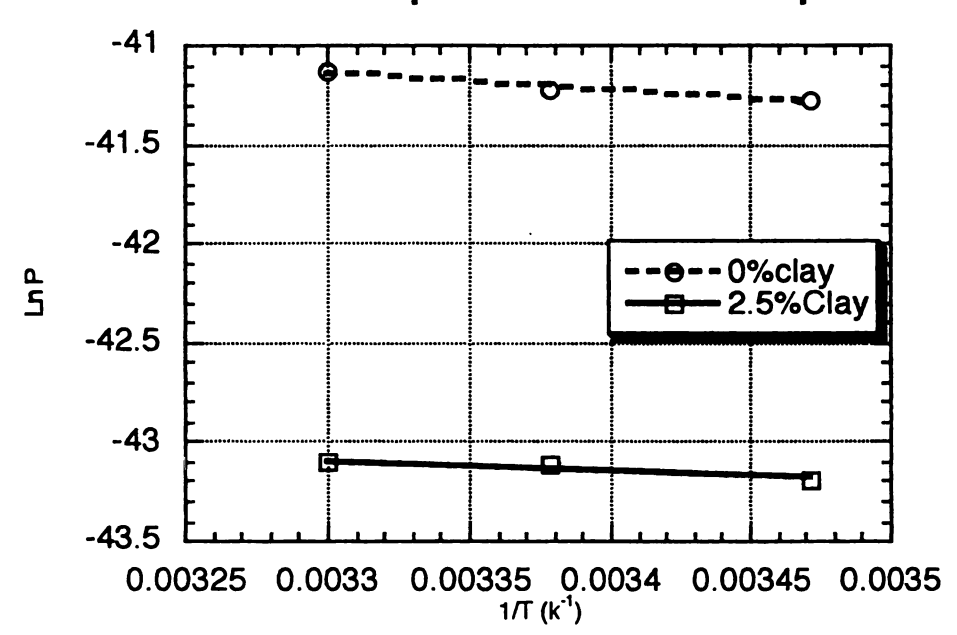
(2) 2.5% Clay polyimide

Ln P = 
$$-41.488-487.75/T$$
, R =  $0.93888$ 

The calculated activation energies are, 7.118 KJol/mol (1.702 KCal/mol) for the 0% clay loading film, and 4.053 KJol/mol (0.97 KCal/mol) for the 2.5% clay loading film, respectively.

The activation energy values for ethyl acetate permeability were quite low, as compared with activation energy values determined for ethyl acetate permeability through selected commodity polymers (see Table 11),

Figure 11. Ethyl Acetate Permeability and Temperature Relationship



illustrating the lack of a significant temperature dependence of the mass transfer process over the temperature range evaluated. As discussed above, this behavior is typical of glassy polymers. In this case, the test temperatures were

Table 11. Activation Energy Values for the Permeation of Ethyl Acetate through Polymer Films Reported in Literature<sup>(a)</sup>

Polymer Membranes	Ea (KJol/mole)
HDPE	41.50
OPP	83.38
Saran Coated OPP	102.84
Acrylic Coated OPP	100.57
Glassine	69.19
0% Clay/Polyimide	7.1 <sup>(b)</sup>
2.5%(v/v) Clay/Polyimde	4.1(b)

(a)Determineded at an ethyl acetate vapor activity of 0.095 (Huang, 1996) (b)Determined in this study

far below the Tg of the polyimide, which is 399 °C (Sykes and St.Clair,1986). When the polymer is at a temperature well below its Tg, polymer chains are less flexible, and the free volume paths available for permeant diffusion are fixed. So the permeability coefficient is quite constant at test temperatures below  $T_{\rm g}$ .

3. The Effect of Ethyl Acetate Vapor Pressure on the Permeability of Polyimide Film with and without Clay Inclusion

The effect of organic vapor concentration on the permeability of polyimide films with and without clay loading was evaluated at two penetrant partial pressure levels. For each partial pressure value, studies were carried out at three temperatures. The results are summarized in Table 12.

Table 12. Effect of Ethyl Acetate Vapor Pressure on the

Permeability of Clay/Polyimide Composite Films

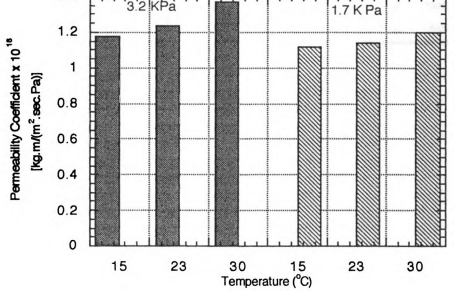
		COMPODICE LILING	
Ethyl Acetate Partial Pressure (KPa)	Test Temperature (°C)	Permeability Coefficient x 10 <sup>18</sup> [kg.m / (m <sup>2</sup> .sec.Pa )] <sup>(a)</sup>	
		0% v/v Clay	2.5%v/v Clay
3.2	15	1.18	0.175
(24.36 mmHg)	23	1.24	0.188
	30	1.37	0.190
1.7	15	1.12	0.134
(12.87 mmHg)	23	1.14	0.127
	30	1.20	0.148

<sup>(</sup>a) Each Value is the average of replicate analyses

The above results show that the organic vapor concentration did not significantly affect the permeability coefficient values for the respective polyimide films. From Table 12, it is apparant that when the organic vapor concentration is reduced from 3.2 KPa to 1.6 KPa, there is very little observed change in the permeability coefficient values of either film. The effect of temperature and vapor pressure on the barrier characteristics of the nanocomposite films is illustrated in the histograms presented in Figures 12. and 13, respectively.

Figure 12. The Effect of Organic Vapor Pressure and Temperature on the Permeability of 0% Clay Polyimide Film

1.4
1.2
1



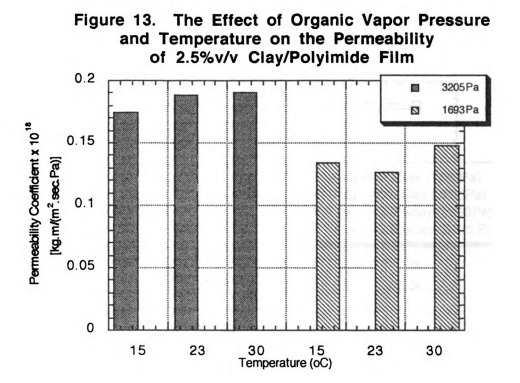
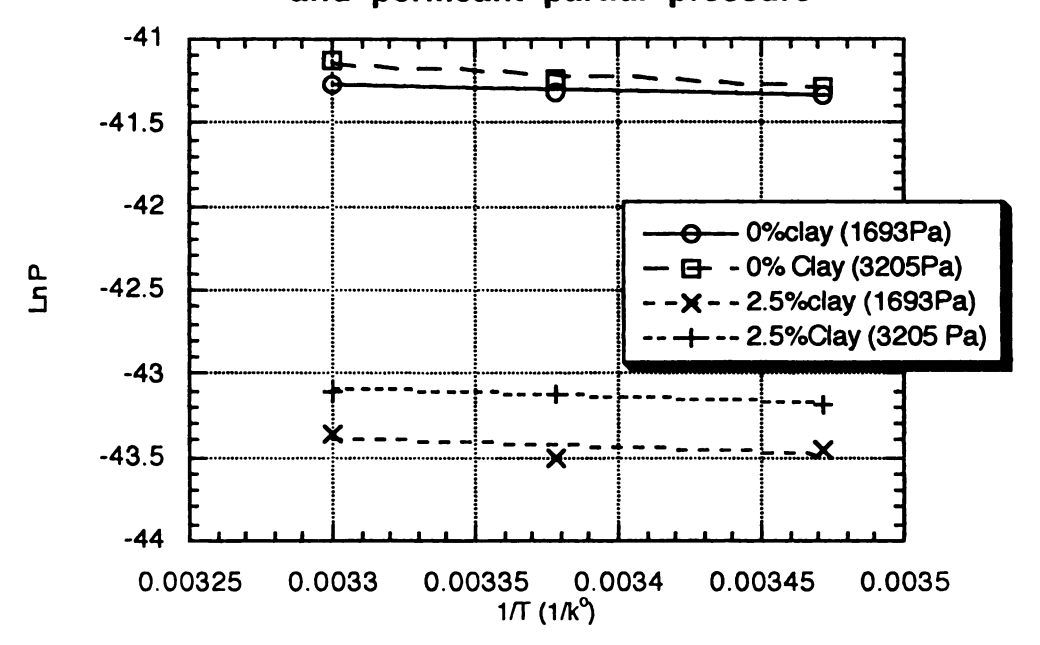


Figure 14. Arrhenius Plot of Ethyl Acetate Permeability as a Function of Clay Loading and permeant partial pressure



The effect of both organic vapor pressure and temperature on the permeability of ethyl acetate through clay/polyimide films is illustrated in Figure 14, where the permeability coefficient is plotted as a function of temperature  $[1/T({}^{\circ}K)]$  for studies carried out at  $\Delta p = 1.7$  and 3.2 KPa. As can be seen, the temperature dependency of the transport values, over the temperature range studied, follows the Arrhenius relationship. From the slopes of the Arrhenius plots, the activation energy values at the test permeant vapor pressure (Ep) level were determined for the respective permeant/polymer systems. The values are summarized in Table 13.

Table 13. Activation Energies at Different Vapor Pressures

Organic Vapor Pressure (KPa)	Activation Energy (KJol/mol)	
	0% v/v Clay	2.5%v/v Clay
3.2	7.1	4.1
1.7	3.3	4.5

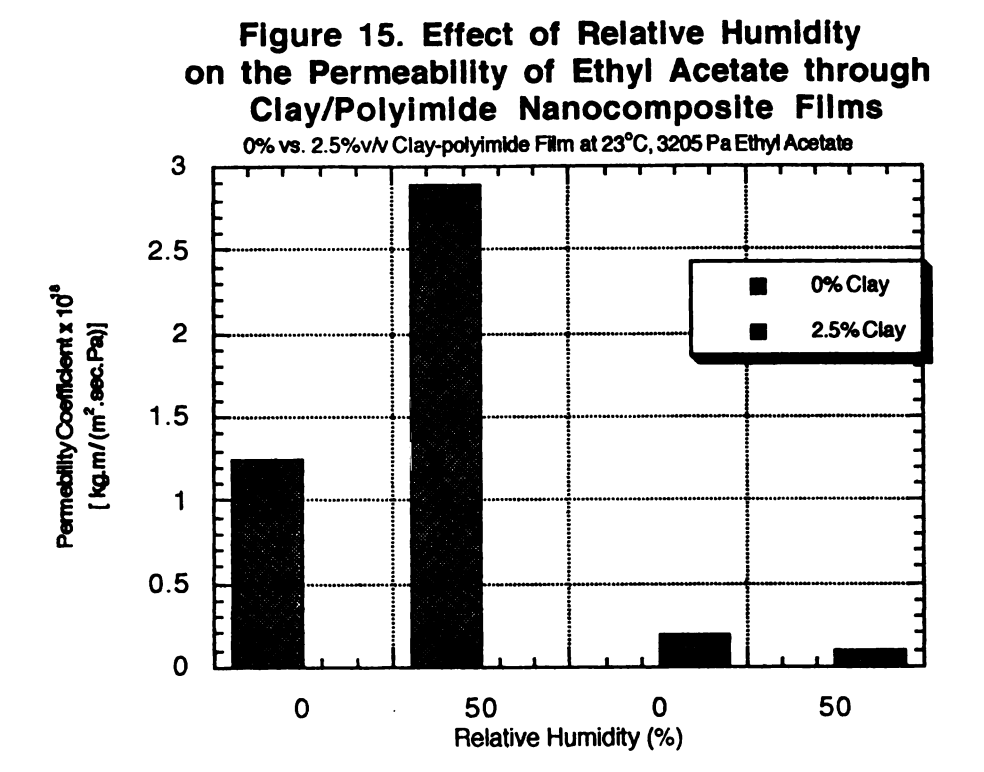
The results presented in Table 13, indicate that the activation energy for the clay/polyimide composite film was not affected by the change of penetrant vapor pressure, while the activation energy of the pure polyimide showed a minimal dependency on penetrant concentration.

When tested under dry conditions, there was no observed effect of repeated exposure to the organic vapor on the barrier properties of the respective polyimide and clay/polyimide structures. Thus, no apparant morphological

changes were indicated as a result of sorption of ethyl acetate by the test films. The sorbed ethyl acetate can thus be totally outgassed and similar permeability coefficient values obtained on repeated analysis of the same film. The relatively constant activation energy values exhibited by the two structures, to different organic vapor pressures, provide further evidence of their chemical resistance.

# 4. The Effect of Relative Humidity on the Permeability of Ethyl Acetate Through Polyimide Films with and without Clay Inclusion

The effect of sorbed water on the permeability of ethyl acetate through polyimide-clay films was measureed by setting the relative humidity of the permeant vapor at 50%RH and performing permeability studies at 23 °C and an organic vapor pressure of 3.2 KPa. In order to minimize the variation of the transmission rate due to the fluctuation of the FID signal under wet test conditions, six measurements were carried out for each structure. The results are reported as averages and the standard deviations, and are summarized in Table 14. As shown, an increase in the permeability coefficient for the pure polyimide film was observed with an increase in relative humidity, while a significant reduction in the permeation rate was observed for the film with 2.5% clay loading, as compared to the results determined at dry condition. A graphical presentation of the permeability



values obtained under dry and humidified conditions is shown in Figure 15.

The observed increase in the permeability values observed for the film without clay may result from the interaction of water vapor with the polymer. Previous permeability studies carried out on the polyimide films showed a very high WVTR value for this film (Table 1). It is therefore, considered a poor moisture barrier.

Table 14. Effect of Relative Humidity on Ethyl Acetate Permeability of Clay/Polyimide Films

1011104021217 01 024771027211240 122115			
Relative Humidity	Permeability Coefficient x 10 <sup>18 (a)</sup> [kg.m / (m <sup>2</sup> .sec.Pa )]		
	0%v/v Clay 2.5% v/v Clay		
0	Avg. 1.24 ± 0.03	Avg. 0.19 ± 0.002	
50	Avg.(b) 2.89	Avg.(b) 0.09	
	Std.dev. 0.92	Std.dev. 0.03	

(a) Tested at 23 °C, 3.2 KPa ethyl acetate vapor pressure

Although the polyimide film exhibited a low permeability to ethyl acetate, when compared to the permeability of a commodity film such as polypropylene [P = 2.0 x 10 -17 kg.m/(m².sec.Pa )](Huang, 1996), the sorbed water may plasticize the film, which can lead to a pathway that allows for a higher rate of diffusion for organic molecules. Sorption of moisture by the polyimide film, can thus account for the observed increase in the permeation rate of the organic vapor under humidified conditions. Such an effect of relative humidity on the barrier properties of the polyimide structure studied is not unexpected and precedence for such

<sup>(</sup>b) Average of six replicate analyses

behaviour in polymers with an affinity for water is found in the literature (Barrie, J.A., 1968; Meyer, J.A.et al., 1957; Ito, 1961; Petrak, 1980; Long, 1953)

Reduction in the organic vapor permeability of the film containing clay is not fully understood, but may result from a reduction in the solubility or diffusivity of the organic vapor in the clay/polyimide nanocomposites. In the clay-polyimide structure, there are a number of Si-O and Al-O groups, which can readily interact with sorbed water vapor. Assuming there is a competitive sorption between H<sub>2</sub>O and ethyl acetate for active sorption sites, when more active sites are occupied by H<sub>2</sub>O, the solubility of organic vapor will decrease.

Landois-Garza and Hotchkiss (1988) reported an example of an increase in the effectiveness as a barrier of a polyvinyl alcohol (PVOH) film with increasing relative humidity for the penetrant, ethyl propionate. The authors explained the observed decrease in permeation, as relative humidity increases, in terms of the change in diffusion (D) and solubility (S) coefficient values as a function of relative humidity. For this system, diffusion coefficient values remained relatively constant, but at high relative humidity showed a slightly downward trend. Solubility coefficient, however, showed a clear trend toward lower solubility at high relative humidity. The authors thus concluded that the decrease in P as relative humidity

increases was mainly the result of the decrease in penetrant solubility.

Hernandez (1994) studied the effect of sorbed moisture on the permeability coefficient of oxygen through an amorphous Nylon (Nylon 6I/6T). Values of the oxygen permeability decreased sharply in the range of water activity from 0 to 0.20 at 11.9 °C and 22 °C, and from 0 to near 0.45 at 40.3 °C. Further studies showed that the diffusion coefficient tended to increase as the moisture content in Nylon 6I/6T increased, and there was a rapid decrease in solubility values when the water activity range was between 0 to 0.2. Based on these findings, the author proposed that the combined effect of sorbed water on both the diffusion and solubility coefficients must account for the net decrease in the permeability of oxygen as a function of sorbed water vapor.

# 5. Estimation of Diffusion Coefficient Values for Ethyl Acetate Through Polyimide and 2.5%(v/v) Clay Polyimide Films

In addition to the permeability coefficient, the isostatic permeability technique also allows determination of diffusion coefficient values. Tables 15.1 and 15.2 summarize the diffusion coefficient values obtained for both non-clay loading polyimide and 2.5%(v/v) clay/polyimide nanocomposite films. The procedure followed for determining the diffusion

coefficient values is discribed in detail in Appendix A. Further, inherent sources of error associated with the

Table 15.1. Diffusion Coefficients for 0% Clay/Polyimide Films

Ethyl Acetate Vapor Pressure (KPa)	Test Temperature (°C)	Diffusion Coefficient x 10 <sup>14</sup> (m <sup>2</sup> /sec) <sup>(a)(b)</sup>
3.2	15	6.0 ± 2.2
	23	3.1 ± 0.2
	30	2.8 <sup>(c)</sup>
1.7	15	6.1 ± 2.2
	23	5.7 ± 1.3
	30	2.9 <sup>(d)</sup>

- (a) Average of replicate runs
- (b) Determined by the baseline subtracting method (See Appendix A)
- (c) One measurement
- (d) At two significant figures, no measurable deviation from mean was calculated for replicate analyses

Table 15.2. Diffusion Coefficients for 2.5%(v/v) Clay/Polyimide Nanocomposite Films

Ethyl Acetate Vapor Pressure	Test Temperature (°C)	Diffusion Coefficient x 10 <sup>13</sup> (m <sup>2</sup> /sec) <sup>(a)(b)</sup>
(KPa)		
3.2	15	1.8 ± 0.3
	23	2.5 ± 0.1
	30	2.4 ± 0.7
1.7	15	1.8 ± 0.1
	23	1.4 ± 0.2
	30	2.2 ± 0.4

- (a) Average of replicate runs
- (b) Determined by the baseline subtraction method (See Appendix A)

diffusion coefficients determined for high barrier structures, such as the clay/polyimde nanocomposites, are described in the Error Analysis Section.

DeLassus (1993) proposed that the high barrier properties of glassy polymers to organic penetrants such as flavor, aroma and solvent molecules can be attributed to the low diffusion coefficient values for these penetrant/polymer systems. Typically, these values are too low to be measured by standard analytical procedures and are less than 10-17 m<sup>2</sup>/sec, or possibly orders of magnitude lower. The diffusion coefficient determines the dynamics of the permeation process and thus the time to reach steady state, which accounts for glassy polymers exhibiting high barrier characteristics to organic permeants. Polyolefins, being well above their glass transition temperature, are non-glassy polymers and have high diffusion coefficients for organic permeants, and steady state permeation is established quickly in such structures.

Comparison of the Diffusion of Ethyl Acetate at Table 16.

Low Vapor Avtivities in Polymers

Polymer Structure	Diffusion Coefficient x 10 <sup>14</sup> ( m <sup>2</sup> /sec)
High Density Polyethylene(a)	4.0
Oriented Polypropylene(a)	3.0
Saran Coated OPP <sup>(a)</sup>	0.16(b)
Polyimide <sup>(c)</sup>	2.9
2.5%(v/v) Clay/Polyimide(c)	22

<sup>(</sup>a) Tested at 30 °C (Huang, 1996)

<sup>(</sup>b) Apparent diffusion coefficient, representative of the structure

<sup>(</sup>c) Tested at 30 °C (This study)

Table 16 lists the diffusion coefficients for ethyl acetate in several commodity polymers. Table 16 also contains the diffusion coefficient values for the clay and non-clay polyimide films investigated in the present study. The polyolefin films show high diffusion coefficients, which is consistent with their high permeation rates to ethyl acetate vapor (Huang, 1996). The Saran coated OPP structure has the lowest diffusion coefficient, which is consistent with its low ethyl acetate permeability (Huang, 1996).

As described above, glassy polymers typically have low diffusion and permeability coefficients for organic penetrants at low vapor concentrations. However, from Table 15.1 and 15.2, it becomes evident that the polyimide films, with and without clay loading, behave atypically in that these films exhibit high diffusion coefficients, comparable to the polyolefins, and low organic vapor permeability rates.

Assuming the relationship given by the Equation:

$$P = D.S \tag{5}$$

is valid, a possible explanation for the low permeability coefficient and high diffusion coefficient values obtained for the respective ethyl acetate/polyimide systems may lie with the low solubility of ethyl acetate in the polyimide film structures.

#### ERROR ANALYSIS

The errors in the experiments of this study can come from several sources, which include the uniformity of the test films which is related to the film processing, as well as measurement errors and uncertainties from the test procedures.

First, the uniformity of the test films introduced the most variation in this study. Each sample of film was prepared by an individual batch procedure. Even for the pure polyimide films, variations may occur when using polymer solutions from a different condensation polymerization series. In addition, when preparing clay/polyimide composites, variation in stirring efficiencies in the reaction vials may result in different aspect ratios for the clay particles. Finally, each film was cast on individual glass plates. Differences in surface properties of the respective glass plates may result in variation of film thickness. All of these variables can contribute to differences in the individual film samples in terms of the film thickness (estimated 10%), and aspect ratio of the clay particles (hard to be estimated), and can account for the variation observed for the permeability values and the apparant aspect ratio values.

Secondly, the instrumental measurements can introduce specific errors. For the WVTR testing, the errors and uncertainty can come from: (1) the purity of the salt used to prepare the saturated salt solutions, which may affect the headspace driving force (estimated 1%); (2) The variation of the steady state transmission rate values (estimated 3%); (3) The precision of the voltmeter (1%); The thickness variation (10%). The estimated compound error of the permeability coefficient value was approximatly 15%.

For oxygen transmission rate testing, since instrument parameters and detector signal output are controlled by a computer and the temperature control bath is well controlled, variations from steady state transmission rate is limited (estimated 1%). The thickness variation was the same as above(10%). In this specific study, an additional concern may be the concentration of the test gas, which contains 2% oxygen (estimated error 5%). At such a low concentration level, any inaccuracy would have a significant influnce on the permeability. The estimated compound error was approxmatly 16%.

For  $CO_2$  testing, variation in test temperatures could be an issue since the test were carried out at room temperature(i.e.  $25\pm3$  °C). Any variation in room temperature would result in variation of the transmition rate (estimated 3%). The graphic calculation is estimated to introduce an error of 1%. The thickness variation was the same as

described above. The compound error is therefore estimated at 14%.

For ethyl acetate vapor permeability testing, there are several sources which may result in errors. First, the actual partial pressure of ethyl acetate in the test gas may not be exactly equal to the assumed value, which is the saturation vapor pressure generated in the sparger. If there is a variation between the assumed and actual vapor pressure, the actual vapor pressure will be somewhat lower than the assumed value. It is difficult to estimate quantitatively the variation between the assumed and actual vapor pressure values, without an external calibration. The temperature variation of the sparger bath (±1 °C) can affect the actual organic vapor pressure (estimated 4%). Secondly, the steady state transmission rate values showed a variation of about 3% for testing at dry conditions and 5% for testing at wet conditions. Thickness variation was the same as described above (estimated 10%). The estimated compound error for the permeability coefficients was about 17% for the dry test and 19% for the wet test, when using the Saturated/Differential (S/D) mode.

To determine the diffusion coefficient from a permeability experiment with the Aromatran 1A system, the instrument must be operated in the Void/Differential (VD) mode (see Literature Review). This requires the outgassing of any pe-absorbed residual organic volatiles before the test run is initiated. In practice, when the system was switched

from outgassing to testing status, there was a shift in the instrument baseline (i.e. increase in detector output signal), which was included in the detector signal output values used by the instrument software to determine both the permeability and diffusion coefficient values. For poor barrier films, exhibiting high permeation rates, this shift or "jump" in the baseline would be minimal and would not introduce significant error to the determined permeability and diffusion coefficient values. However, for films with very low permeability values, such as the clay/polyimide composite film, such a shift in the baseline could greatly affect the accuracy of the test results. Since determination of the diffusion coefficient is based on the "half-time" method, this shift in the baseline can result in an over estimation of the diffusion coefficient value, as well as contribute to error in the permeability coefficient values determined, partically for high barrier structures. Because of these considerations, in the present study, the Saturated/Differential (SD) procedure was used for accurate determination of permeability coefficient values, while the Void/Differential (VD) procedure was used to estimate the diffusion coefficients. As described in Appendix A, the detector output signal was corrected from the shift in baseline and the diffusion coefficient values were then determined. An estimated compound error for the diffusion coefficient values was about 17% for the studies carried out under non-humidified conditions.

## SUMMARY AND CONCLUSIONS

The permeability of water vapor, oxygen, carbon dioxide, and ethyl acetate vapor through clay/polyimide nanocomposite films was determined with the MOCON Permeatran-W, Ox-Tran 200, Permatran C-IV, and the Aromatran 1A permeability testers, respectively. Factors affecting the barrier properties of clay/polyimide nanocomposites including the following: (i) the clay loading level; (ii) the test temperature; (iii) the organic vapor concentration; and (iv) the relative humidity, were evaluated.

Based on the results presented in the previous sections, the conclusions which can be drawn from the study are summarized below:

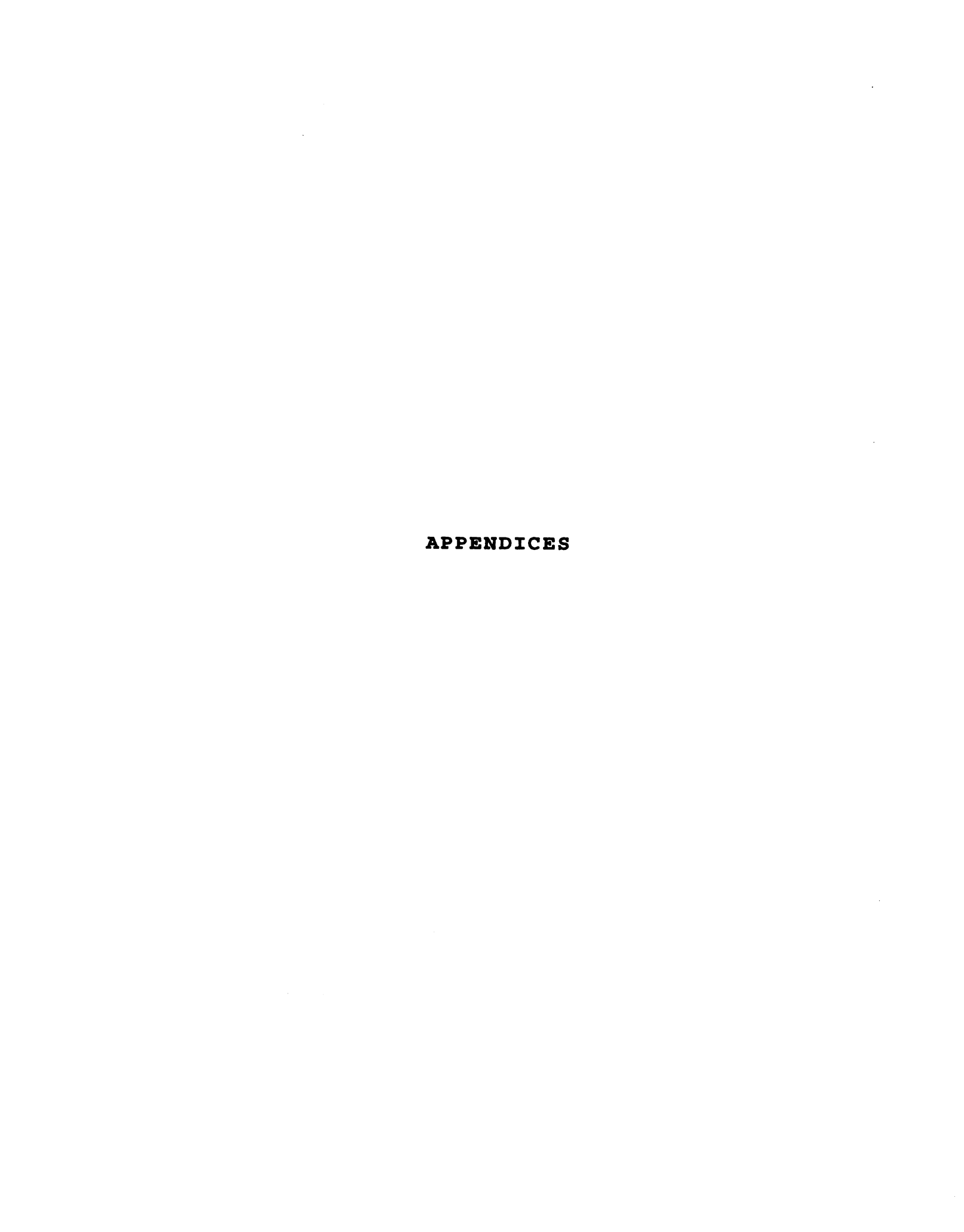
- 1. The mass transfer process for the respective penetrants, i.e.  $H_2O$ ,  $CO_2$  and  $O_2$ , is highly dependent on the clay loading level and exhibits a non-linear dependency with respect to the decrease in permeability. With a clay loading level of 2.5%(v/v), the permeability coefficients to  $H_2O$ ,  $O_2$  and  $CO_2$  were reduced to 39%, 47% and 54% of the permeability value of the pure polyimide.
- 2. The temperature dependency of the transport process for oxygen, over the temperature range studied (0-30 °C), followed well the Arrhenius relationship. The obtained

activation energies for the pure polyimide and the 2.5%v/v clay/polyimide are 16.9 KJol/mol and 19.6 KJol/mol, respectively.

- 3. The width-to-thickness ratios or the apparent aspect ratios for the clay particles were estimated to be within the range of 83-132, which increased the total path of the diffusing gas and resulted in a non-linear decrease in permeability values.
- 4. For ethyl acetate as penetrant, the following results were obtained:
- (a) When tested at dry conditions, the polyimide with the 2.5%v/v clay loading exhibited enhanced barrier properties to ethyl acetate vapor when compared to the pure polyimide film. The clay/polyimide nanocomposite film showed an 85% reduction in the permeability coefficient, when compared to the polyimide film without clay loading.
- (b) Within the test temperature range from 15℃ to 30 ℃, the effect of temperature on the permeability coefficients is minimal. When tested at 3.2 KPa ethyl acetate vapor pressure, the activation energies for the pure polyimide and the 2.5%v/v clay/polyimide are 7.1 KJol/mol and 4.1 KJol/mol, respectively.
- (c) Over an ethyl acetate vapor pressure range from 1.7 KPa to 3.2 KPa, the permeability coefficient appears to be independent of vapor concentration. There was no indicated effect of penetrant vapor pressure on the activation energies for the clay/polyimide composite film, while the activation

energy of the pure polyimide showed a minimal dependency on penetrant concentration.

- (d) When moisture (50% RH) was introduced to the test system, the permeability coefficient value of the pure polyimide film increased by one hundred percent as compared to the permeability coefficient value determined under dry conditions. However, the permeability coefficient for the clay/polyimide nanocomposite (2.5%v/v) film showed a decrease of approximately 50% when determined under humidified conditions.
- (e) The low permeability but high diffusivity makes the polyimide and clay polyimide films a unique property.





#### APPENDIX A

#### Estimation of the Diffusion Coefficient Values

In order to obtain the diffusion profiles of both polyimide and clay/polyimide films to ethyl acetate, it was found necessary to skip the "rezero" setting during the test and to operate the system in the Void/Differential mode. This allowed for acquisition of a sufficient number of data points before the permeation rate reached the equilibrium or steady state level. Since no correction was made for shifting of the baseline, the steady state transmission rate values obtained would not be accurate for films with very low permeability values (see Error Analysis), such as the clay/polyimide composite material. Also, it would introduce errors to the diffusion coefficient values when using the "Half Time Method", since the determination of the half time  $(t_{1/2})$  was related to the equilibrium transmission rate value. It should be pointed out that by operating the system in the Saturated/Differential mode, the "rezero" setting can be applied since in this mode only the steady state permeation rate value, and not the total diffusion profile curve, is to be determined. Thus, permeation rate values obtained in the Saturated/Differential mode, with the "rezero" setting, are assumed to be accurate.

To estimate the diffusion coefficient values more accurately, the following calculations were performed, based on the assumption that the detector output contributed by the shifting of the detector baseline, was a fairly consistent value [around 2000  $\mu g/(m^2.day)$ ]:

- (i) Subtract the transmission rate value associated with the baseline shift from all the data points obtained to generate the diffusion profile curve.
- (ii) Re-plot the diffusion profile curve.
- (iii) Find the value of  $t_{1/2}$ , where the transmission rate value is half of the equilibrium transmission rate value, from the new curve.
- (iv) Use the following formula to get D:

$$D = \frac{l^2}{7.199 \cdot t_{1/2}}$$
 (16)

where l is the thickness of the test film.

Althernatively, the  $t_{1/2}$  value can be determined as follows: i.e. find the  $t_{1/2}$  from the primary curve where the transmission rate  $F_{(half)}$  is:

$$F_{\text{(half)}} = [(F_{\infty} - F_{S})/2] + F_{S}$$

where  $F_{\infty}$  is the transmission rate value at equilibrium state,  $F_S$  is the transmission rate value associated with the baseline shift.

APPENDIX B

## APPENDIX B

## Conversion Between ASTM Units and SI Units

In this study, most results are reported in SI units. In some case, ASTM units are also reported so that we can compare those results with some literature data. The conversion between ASTM units and SI units in terms of permeability coefficients for both gases and vapors are as followings:

# For gases:

 $1 \text{ cc.mil/}(m^2.\text{day.atm}) = 2.94 \times 10^{-21} \text{ m}^3.\text{m/}(m^2.\text{sec.Pa})$ 

# For vapors:

 $1 \text{ g.mil/}(m^2.\text{day.mmHg}) = 2.23 \times 10^{-15} \text{ kg.m/}(m^2.\text{sec.Pa})$ 

BIBLIOGRAPHY

#### **BIBLIOGRAPHY**

- AMCOL International Corporation web page, 1996. "AMCOL Int. Cor. SUM". Web address "http://www.amcol.com". 12/7/1996.
- ASTM, 1988. "Standard Test Method for Oxygen Gas Transmisson Rate Through Plastic Film and Sheeting Using a Coulometric Sensor" ASTM D 3985-81 (reapproved 1988).
- ASTM, 1988. "Standard Testing Method for WVTR of Materials". Annual Book of ASTM Standards. 629.
- Baner, A.L., Hernandez, R.J., Jayaraman, K., Giacin, J.R., 1986. "Isostatic and quasi-isostatic methods for determining the permeability of organic vapors through barrier membranes, Current Technologies in Flexible Packaging", ASTM STP 912: 49-62. American Society for Testing and Materials, Philadelphia.
- Bandosz, T.J., 1992. "Chemical and Structure Properties of Clay Minerals Modified by Inorganic and Organic materials". Clay Minerals, 27,435.
- Barrie, J.A., 1968. "Water in Polymers", in diffusion in Polymers, Edited by J. Crank and G.S. Park, academic Press, New York (1968).
- Berens, AR. and Hopfenberg, L.,1982. "Diffusion of Organic Vapors at Low Concentrations in Glassy PVC, Polystyrene, and PMMA". J. Membrane Sci., (10), 283-303
- Bissot, T.C., 1989. "Barrier Polymers and Structures" ACS Symp. Ser., 423, 225.
- Bonis, L., 1994. "Packaging, plastic outflank traditional materials in growth and market share", Modern Plastic Encyclopedia '94. 28.
- Blumstein, A., 1965. "Polymerization of Adsorbed Monolayers. II. Thermal Degradation of the inserted polymer". J. Polym. Sci., Part A.3, 2665
- Blumstein, R., 1974. "Acrylonitrile in Macromolecules"., Apply. Polym. Symp., 25, p.81, Chicago, August, 1974.

Brody, A.L., 1993, "Glass-coated Flexible Film for Packaging", Packaging Technology and Engneering, March 1993.

Caldecourt, V. and Tou, J., 1985. "Atmospheric Pressure Ionization Mass Spectrometeric and Photoionization Techniques for Evaluation of Barrier Film Permeation Properties". TAPPI Proceedings: Polymers, Laminations and Coatings Conference. 441-444.

Chang, Y., 1996. Organic Vapor Permeability of High Barrier Polymer Membranes by a Dynamic Purge and Trap/Thermal Desorption Procedure. Master's Thesis, School of Packaging, Michigan State University.

Choy, C.L., Leung, W.P., and Ma, T.L., 1984. "Sorption and Diffusion of Toluene in Highly Oriented Polypropylene". J. polymer Sci,, Polymer Physics Edition, (22), 707-719.

Crank, J., and Park, S.G., 1968. "Diffusion in Polymers". Academic Press, New York, NY.

Crank, J., 1975. "The Mathematics of Diffusion." Clarendon Press, Oxford, England.

Critchley, J.P. and Wright, W.W., 1979. "Polyimide as Matrix Resins for Composites", Reviews on High-Temperature Materials, Vol.IV, No.2, 108

Delassus, P.T. 1993. "Permeation of Flavors and Aromas through Glassy Polymers". Polymers, Laminations & Coatings Conference, No.1, 236-266.

DeLassus, P.T., 1985. "Transport of Unusual Molecules in Polymer Films". Polymers, Laminations & Coatings Conference / TAPPI Proceedings, 445

Demorest, R.L., 1995. "Measurement of Water Vapor Permeability: Recent Developments and New Standards". Presentes at PACKFORSK SYMPOSIUM, Stockholm, Sweden, March 23, 1995.

Dirienzo, H.A., 1993, "What Is a High Barrier Package?" Polymer, Laminations & Coatings Conference, TAPPI Proceedings. 251-253.

Felts, J.T., 1993., "Transparant Barrier Coatings Update", Plastic Film & Sheeting", V.9, 139

Ford, T., 1995, "New Material Keeps Oxygen out of Packages", Plastic News, Sept.25.

Fukushima, Y.; Inagaki, S., 1987. "Snthesis of an Intercalated Compound of Montmorillonite and 6-Polyamide". J. Inclusion Phenom., 5, 473.

Fukushima, Y., Okada, A., Kawasumi, M., Kurauchi, T., and Kamigaito, O., 1988. "Swelling Behaviour of Montmorillonite by Poly-6-Amide". Clay Miner. v.23, 27

Giacin, J. R., 1994. PKG 815 Course Pack, Michigan State University

Giannelis, E.P, 1992(a). "A new strategy for synthesizing polymer-ceramic nanocomposites". JOM, vol. 44, 28

Giannelis, E.P., Mehrotra, V.; Tse, O.; Vaia, R. A.; and Sung, T.-C., 1992(b). "Intercalated two-dimesional ceramic nanocomposites". Mat. Res. Soc. Symp. Proc. Vl. 267, 969-80

Goff, D. and Yuan, E., 1988. "Approaches to organic dielectrics with reduced moisture absorption and improved electrical properties". Polym. Mater. Sci. Eng., v.59, 186.

Greenland, D.J., 1963. "Adsorptions of Polyvinyl Alcols by Montmorillonite". J.Colloid Sci, 18, 647.

Hernandez, R.J. and Giacin, J.R., 1997. Chapter 10 of Quality Preservation In Food Storage & Distribution, Edited by Taub, I., Singh, R.P., CSC Press.

Hernandez, R.J., 1994. "Effect of water vapor on the transport properties of oxygen through polyamide packaging materials". J. of Food Engineering 22, 495-507.

Hernandez, R.J., Giacin, J.R. and Baner, A.L., 1986. "The evaluation of the aroma barrier properties of polymer films". J. Plastic Film and Sheeting, 2 (3), 187-211.

Huang, S.,1996. "Evaluation Isostatic and Quasi-Isostatic Precedures for Determining the Organic Vapor Barrier Properties through Polymer Membranes". Master's Thesis, School of Packaging, Michigan State University.

Imi-Tech® Corporation's web site "http://www.imitech.com".

Ito, Y., 1961. "Effect of water vapor on permeation of gases through hydrophilic polymers". Chem. High Polym. Jn 18, 158.

Kato, C., Kuroda, K., Misawa, M., 1979. "preparation of montmorillonite-nylon complexes and their thermal properties". Clays Clay Miner., v.27, 129-136.

Krishnamoorti, R., 1996. "Structure and Dynamics of Polymer-layered Silicated Nanocomposites", Chem. Mater., 8, 1728-1734

Labadie, J and Hedrick, J., 1990. "New Low Dielectric Constant Polyimide Block and Random copolymers". Soc. Adv. Mater. Process Eng. J., 26(4), 19.

Lagaly, G.and Beneke, K,, 1975. "Intercalation and Exchange Reactions of Clay Minerals and Non-clay Layer Compounds". Am. Mineralogist, 60, 650-658

Lan, T. and Pinnavaia T.J., 1994(a). "On the Nature of Polyimide-Clay Hybrid Composites", Chemistry of MATERIALS, Am. Chem. Soc., No.6, 573

Lan, T. and Pinnavaia, T.J., 1994 (b). "Clay-Reinforced Epoxy Nanocomposites". Chem. Mater. 6, 2216-2219

Lan, T., 1994(c). Doctoral Dissertation. Chemistry Department, Michigan State University

Lan, T., 1996. Personal telephone interview with Dr. Lan T., Research Scientist, Nanocor, Inc., 12/7/1996

Landois-Garza, J. and Hotchkiss, J.H., 1988. "Permeation of High-barrier Films by Ethyl Esters, Food and Packaging Interactions", Chapter 4, Edited by J.H. Hotchikiss, American Chemical Society.

Lin, C.L., Lee, T. and Pinnavaia, T.J., 1992. "Supromolecular Architecture: Synthetic Control in thin films and Solids". ACS Symp. Ser., 499, 145

Loebig, C., 1996. Personal telephone interview, July, 1996.

Long, F.A., and Thompson, L.J., 1953. "Water induced acceleration of the diffusion of organic vapors in polymers". J. Polym. Sci. 8, 321.

MAS Technologies Product brochures:

- (1) MAS 1000 Moisture Permeation Sysytem
- (2) MAS 2000 Organic Permeation Detector
- (3) MAS 500 Oxygen Diffusion System

Maul, P., 1995. "Company Formed to Develop High Barrier Plastic 'Nanocomposites'", Packaging Strategies, August 31, 1995.

Meares, P., 1965. "Transient Permeation of Organic Vapors through Polymer Membranes". J. of Applied Polymer Science, Vol.9, 917-932.

Mehrotra, V., Giannelis, E.P., 1990. "Polymer Based Molecular Composites", MRS Symp. Proc., D.W. Schaefer J.E. Mark, Eds., MRS. Pittsburgh, 171.

Messersmith, P.B. and Giannelis, E.P., 1993. "Polymer-layered silicate nanocomposites". Chem. Mater. 5, 1064-1066

Messersmith, P.B., and Giannelis, E.P., 1994. "Synthesis and Characterization of Layered Silicate-Epoxy Nanocompoites". Chem. Mater. 6, 1719-1725

Messersmith, P.B., Giannelis, E.P., 1995. "Synthesis and Barrier Properties of Poly( $\varepsilon$ -Caprolactone)-Layered Silicate Nanocomposites". J. Polym. Sci., A: Polym. Chem., 33(7), 1047-1057.

Meyer, J.A., Rogers, C., Stannett, V. and Szwarc, M., 1957. "Studies in the gas and vapor permeability of plastic films and coated papers PartIII. The permeation of mixed gases and vapors". TAPPI, 40, 142

MOCON web page, 1996. Web address: "http://www.mocon.com"

MOCON, 1982. Operating Manual for Permatran-W. 7500 Boone Avenue North, Minneapolis, Minnesota 55428 USA.

MOCON, 1983. Operating Manual for Permatran C-IV.

MOCON, 1989. Oxygen Permeation System Operating Manual.

MOCON, 1996. Permatran-W 3/31 operator's Manual.

MOCON, 1996. Aromatran-1A Operator's Manual, preliminary.

Mohney, S.M., Hernandez, R.J., Giacin, J.R., Harte, B.R.Miltz, J., 1988. "The Permeability and Solubility of d-Limonene Vapor in Cereal Package Liners". J. Food Sci., 53, 253.

Murty, N.S., Kotliar, A.M., and Sacks, W., 1986. "Structure and Properties of Talc-Filled Polyethylene and Nylon 6 Films" J. of Applied Polymer Science, 31, 2569.

Nanocor web page, 1996. "Nanocomposites". Web address "http://www.nanocor.com". 12/7/1996

Neilsen, L.E., 1967. "Models for the permeability of filled polymers". J. Macromol. Sci. (Chem.), A1(5) 929-942.

Okada, A., Kawasumi, M., Usuki, A., Kojima, Y., Kurauchi, T., and Kamigaito, O., 1989. "Polymer Based Molecular Composites". MRS Proceedings: Boston, MA, 45.

Okada, A., Kawasumi, M., Usuki, A., Kojima, Y., Kurauchi, T., and Kamigaito, O., 1990. Mat. Res. Soc. Symp. Proc. 171, 45-50

- Packaging World Staffs, PackExpo1996. "Packaging 2000 Profiles", Reprint from Packaging World, Oct. & Nov. 1995.
- Pasternak, R. A., Schimscheimer, J.F., and Heller, J., 1970. A Dynamic Approach to Diffusion and Measurements. J. Polymer Sci., Part A-2, 8, 467-479
- Petrak, K., and Pitts, E., 1980. "Permeability of Oxygen through polymer II, The effect of Humidity and film thickness on the permeation and diffusion coefficients, J. Appl. Polym. Sci., 25, 879
- Pinnavaia, T.J., 1983. "Intercalated Clay Catalysts". Sciense, 220, 365
- Pye, D.G., Hoehn, H.H., and Panar, M., 1976. Measurement of Gas Permeability of Polymers. I. Permeabilities in Constant Volume/Variable Pressure Apparatus., J.Applied Polymer Sci., (20), 1921-1931.
- Rattray, T., 1994. "Source Reduction". Modern plastic Encyclopedia'94, 42.
- Rogers, C.E., 1964. "Permeability and Chemical Resistance of Polymers" in Engineering Design For Plastics. Bear, E. (ed). Rheinhold, N. Y.
- Ruiz-Hitzky, E., 1993. "Conducting Polymers Intercalated in Layered Solids". Adv. Mater. 2(1), 545-547
- Sajiki, T., M.S. Thesis, Michigan State University, East lansing, MI, 1991.
- Seferis, J.C., 1986. "An overview" in Composite Systems From Natural And Synthetic Polymers.. Edited by L. Salmen, et al. Elsevier Science Publishers B.V., Amsterdam.
- Sykes, G.F., and St. Clair, A.K., 1986. "The effect of molecular structure on the gas transmission rates of aromatic polyimide". J. of Applied POlymer Science, Vol.32, 3725
- Stern, S.A., Mi, Y., Yamamoto, H., 1989.
  "Structure/permeability relationships of polyimde membranes.
  Applications to the separation of gas mixtures". J. of
  polymer Science: Part B: Polymer Physics, Vol.27, 1887-1909
- Tohoh, M., 1992. European Patent, 0479031.
- Usuki, A., Okamoto, K., okada, A., Kurauchi, T., 1989. U. S. Patent 4,889,885.
- Usuki, A., Okamoto, K., okada, A., Kurauchi, T., 1995(a). "Synthesis and Properties of Acrylic Resin-Clay Hybrid".

Japanese Journal of Polymer Science and Technology. V.52, No. 11, 727-733.

Usuki, A., Koiwai, A., Kojima, Y., Okada, A., 1995(b). "Interaction of Nylon 6-clay surface and mechanical properties of nylon 6-clay hybrid". J. of Applied polymer Sci., v.5, No.1, 119-123.

Vaia, R.A., Ishii, H. and Giannelis, E.P., 1993. "Synthesis and properties of two-dimensional nanostructures by direct intercalation of polymer melts in layered silicates". Chem. Mater., v.5, 1694-1696.

Vieth, W.R. 1991. Diffusion In And Through Polymers. Oxford University Press, New York

Watanabe, Takehiko, 1987. "Packaging Evaluations of MXD-6 Nylon". Plastic Films & Sheeting, V.3, 215.

Yamamoto, H., et al., 1990. J. of Polymer Science: Part B: Polymer Physics, V.28, 2291-2304.

Yano, K., Usuki, A., Okada, A., Kurauchi, T., Kamigaito, O., 1993. "Synthesis and Properties of Polyimide/Clay Hybrid". J. Polym. Sci: Part A: Polymer Chemistry, V.31, 2493.

Yasuda, H. and Rosengren, K., 1970. "Isobaric Measurement of Gas Permeability of Polymers". J. Applied Polymer Sci, 11(14), 2839.

Ziegel, K.D., Frensdorff, H.K., and Blair,, D.E., 1969. "Measurement of Hydrogen Isotope Transport in Polyvinl Flouride Films by Permeation Rate Method". J. Polymer Sci., A2, 7, 809.

Zobel, M.G.R., 1982, "Measurement of Odour Permeability of Polypropylene Packaging Films at Low Odourant Levels". Polymer Testing, 3, 133.

